UNIVERSITA' DEGLI STUDI DEL MOLISE

DIPARTIMENTO DI BIOSCIENZE E TERRITORIO

_____

DOTTORATO DI RICERCA IN: SCIENZE AGRO-FORESTALI, DELLE TECNOLOGIE AGRO-INDUSTRIALI E DEL TERRITORIO RURALE. I SISTEMI FORESTALI

Ciclo XXVII

COMPARING SINGLE TREE AND AREA BASED APPROACHES FOR BIOMASS ESTIMATION OF CAPE VERDEAN XEROPHYTIC FORESTS USING VISIBLE AERIAL IMAGERY

SETTORE SCIENTIFICO-DISCIPLINARE

AREA 07 AGR/05

COORDINATORE: Chiar.mo Prof. MARCO MARCHETTI

TUTORE: Chiar.mo Prof. GHERARDO CHIRICI

DOTTORANDO: LUCA BERNASCONI

ANNO ACCADEMICO 2015-2016

COORDINATORE: TUTORE:

Chiar.mo Prof. MARCO MARCHETTI   Chiar.mo Prof. GHERARDO CHIRICI

DOTTORANDO: LUCA BERNASCONI

i

ABSTRACT

ITALIAN:

Con base in ortofoto aeree ad alta risoluzione sono stati sviluppati modelli per la stima della biomassa di foreste xerofile capoverdiane.

Il metodo proposto si basa sull'integrazione di tecniche di *clustering* in combinazione con l'indice VARI (Visibile Atmospherically Resistant Index) e algoritmi di segmentazione per l'estrazione chiome degli alberi. Questo procedimento ha permesso la minimizzazione dei problemi dovuti alla scarso contrasto spettrale tra il suolo e le chiome nelle parti più luminose e quelle in ombra.

Sono stati testati metodi basati sul singolo albero e per area (*area based*) e le loro prestazioni sono state contrastate con i dati dell´inventario forestale nazionale di Capo Verde (CV-IFN). Nel primo approccio la biomassa è stata calcolata in funzione della larghezza della chioma e l'altezza degli alberi, utilizzando le equazioni allometriche sviluppate appositamente per l´inventario CV-IFN. Nel secondo approccio si è usata l'analisi di regressione per derivare modelli per la stima della biomassa in funzione dell'area proiettata della chioma.

L´accuratezza delle stime è stata misurata analizzando l´ RMSE (Root Mean Square Error) tra la biomassa stimata e quella osservata.

L´errore osservato nei due modelli è simile, variando tre il 42% del primo approccio e il 45% del secondo.

La biomassa media calcolata per l´intera area di studio (14.399 ettari) con base nei dati del CV-IFN, è di 12,701 Mg ha^{-1}. Questo a fronte di 11,380 Mg ha-1 stimato dal modello per area (area based) e 10,278 Mg ha^{-1} per il modello per singolo albero.

Una stratificazione dell´immagine per aree omogenee, definite da mappe del soprassuolo più precise, può portare a stime di biomassa piú accurate. I modelli proposti aprono spazi per l´applicazione pratica sia a fini di monitoraggio che di gestione delle risorse forestali.

ENGLISH:

Models to estimate the AGB over dry Cape Verdean woodlands were developed using visible high-resolution aerial orthophotography.

The proposed method is based on the integration of clustering techniques combined with the Visible Atmospherically Resistant Index (VARI) and segmentation algorithms for tree crowns extraction. This allowed for the minimization of constraints due to poor spectral contrast between the background and tree crowns, especially for brighter parts of the crowns and shadowed parts of the scene.

Both single tree and area based approaches were tested and their performances compared on the basis of field data from the National Forest Inventory of Cape Verde (CV-NFI). In the first approach, AGB was calculated as a function of crown width and tree height by the allometric equations developed specifically within the CV-NFI. In the second approach, regression analysis was used in deriving models for biomass as a function of the crown projected area.

The accuracy of the values predicted was measured by the Root Mean Square Error (RMSE) against the allometric-based (field-measured) biomass.

The models produced similar accuracy in the AGB predictions with NRMSE% of 42% for the first approach and 45% for the second.

The mean AGB as estimated from the CV-IFN data for the study area of 14399 ha was 12.701 Mg ha^{-1}. This compared with 11.380 Mg ha^{-1} predicted by the area based model and 10.278 Mg ha^{-1} by the single tree model.

The findings demonstrate that promising results can be achieved and as expected, the reliability increases with the area for which mean values are presented. Improvements of the forest maps and the stratification in homogeneous layers can lead to enhanced AGB estimations, something which opens opportunities for the practical application of the models for monitoring and management purposes.

TABLE OF CONTENTS

AD	Absolute deviation
AGB	Above ground biomass
ANN	Artificial neural network
APE	Absolute percentage error
ASL	Airborne Laser Scanner
CHM	Canopy Height Model
CIR	Color-infrared
CPA	Crown projected area
CV-NFI	Cape Verdean National Forest Inventory
DBH	Diameter at breast height
FMDC	Field-Map Data Collector
FMIA	Field-Map Inventory Analyst
GLCM	Gray level co-occurrence matrix
GSSN	Global navigation satellite system
IFER	Institute of Forest Ecosystem Research, Ltd
InSAR	Interferometry SAR
KNN	k-nearest neighbor
LIDAR	Light Detection and Ranging
NFI	National Forestry Inventory
NIR	Near Infrared
NRMSE	Normalized root mean square error
PCA	Principal Component Analysis

Pol-InSAR	Polarimetric SAR Interferometry
RGB	Red Green Blue
RMSE	Root Mean Square Error
RSE	Relative Standard Error
SAR	Synthetic Aperture Radar
SMA	Spectral Mixture Analysis
SVM	Support Vector Machines
SAR	Synthetic Aperture Radar
SE	Standard Error
TCT	Tasseled Cap Transform
VARI	Visible Atmospherically Resistant Index

1. INTRODUCTION

Tree biomass is useful in assessing forest structure and condition to estimate forest productivity and carbon fluxes; in providing a means of assessing sequestration of carbon in wood, leaves, and roots; and also as an indicator of both the biological and economic value of a forest ecosystem. Thus, the estimation of forest biomass at different geographical scales (from local to global) becomes significant in reducing uncertainty of carbon emission and sequestration, measures of land degradation or restoration, and understanding the roles that forests play in environmental processes and sustainability (Foody 2003).

In arid and sub-arid areas, rural populations depend greatly on the sparse scrublands and woodlands for fuelwood and pasture for animals. In such contexts, quick and cost-effective estimation of biomass availability and variation is crucial to implementing proper management practice. This is the case of Cape Verde where, since independence, nationwide campaigns and relevant efforts were realized to promote afforestation of vast arid areas. These woodlands, composed by shrub-like xerophytic trees, although expressing a limited economic value, support significant socio-economic and ecological functions. In this context, the accessibility of simple, fast and inexpensive methods for biomass and forest cover estimation are essential to promoting the monitoring and management of these resources.

The most accurate method by which to estimate forest biomass is based on field measurements, but collection of field measurements is time-consuming and labor-intensive. Moreover, it is impossible to census large geographic areas (Segura and Kanninen 2005; Seidel et al. 2011; Wang et al. 2011), thus it is only suitable for a

small area and cannot provide spatial distribution. Thus, direct collection is generally used to obtain biomass reference data and to develop species-specific allometric models based on measured attributes, such as diameter at breast height (DBH), tree height, crown projected area (CPA) and/or wood density (table 1). Then the allometric models can be used to estimate the AGB for a specific tree, as a function of these parameters for stand biomass inventories.

Methods	Major characteristics	Advantages	Disadvantages	References
Destructive sampling	A tree is cut and dried, and all masses are weighed.	The most accurate approach. An input for development of allometric models.	Destroying trees is time-consuming and labor-intensive and suitable only for small areas.	(e.g. Klinge et al. 1975)
Allometric models	Established for each tree species with linear or nonlinear regression models based on the relationships between biomass and diameter at breast height, tree height, and/or wood density.	Many previous field measurements can be used to calculate biomass.	Not all species have allometric models. Environmental and climatic conditions may affect their applications.	(e.g. Overman et al. 1994; Nelson et al.1999; Henry et al. 2010; Chave et al. 2014)
Conversion from volume	Biomass can be converted from volume at individual tree level or at plot level using volume expansion factor, average wood density, and biomass expansion factor.	Many previous sample plots can be used to calculate biomass.	Species composition and environmental conditions may affect the biomass estimation.	(e.g. Brown and Lugo 1984; Brown et al.1989; Lehtonen et al. 2004; Segura and Kanninen 2005)

Table 1: A summary of major characteristics of biomass calculation from field measurements (adapted from Lu et al. 2014)

Regional or national forest inventories have large tree-volume datasets at plot level and forests stand so the conversion of tree volume to biomass on the basis of the average wood density can greatly reduce time and cost (Lu et al. 2014). However, this approach is not appropriate in woodlands, composed of shrub-like xerophytic

trees, where the ecological and economic interest is focused on the biomass and the measurement of the volume is a challenging task.

A wide range of techniques has been used for biomass estimation. For example, Wang et al. (2009) divided estimation approaches into (1) process model-based; (2) empirical model-based; (3) biomass expansion/conversion factor or coefficient-based; and (4) integration of plot and remotely sensed data (Lu et al. 2014).

Process-based ecosystem models employ biogeochemical processes, including photosynthesis, absorption, and carbon allocation. The models generally include biology, soil, climate, hydrology, and anthropogenic effects (Smyth et al. 2013). Constraints in data source (e.g. climate data, soil, and topography), spatial resolution, and inaccuracy of models often result in high uncertainties in biomass estimates (Rivington et al. 2006; Zhang et al. 2012). Process-based ecosystem models assume homogeneous stands and lack the ability to provide spatial variability in forest biomass. Conversely, remote sensing has the capability to consistently capture land surface features over large areas. (Lu et al. 2014).

In past decades, an increasing number of researches have explored the suitability and applied remote sensing-based models to provide accurate biomass estimation across different ecosystems and at different geographical scales.

Remotely sensed data collected by optical multispectral and hyperspectral sensor, radar and Lidar combined with techniques based on empirical regression models and nonparametric algorithms are commonly used to estimate above ground biomass (AGB) of forested landscapes (Goetz et al. 2009), (Gleason and Im 2011), (Katoh and Gougeon 2012), (Vaglio Laurin et al. 2014), (Huang, Y. P., and J. S. Chen.

2013), (Hudak, A. T., et al, 2012), (Muukkonen and Heiskanen 2007; Blackard et al. 2008; García et al. 2010; Mitchard et al. 2011) (table 2).

Category	Variables	Description	References
Optical sensor data	Spectral features	Spectral bands, vegetation indices, and transformed images	(e.g. Foody et al. 2003; Zheng et al.2004)
	Spatial features	Textural images and segments from the spectral bands	(e.g. Lu and Batistella 2005)
	Subpixel features	Fractional features such as green vegetation and NPV by unmixing the multispectral image	(e.g. Lu et al. 2005)
	Combination of spectral and spatial features	Combination of images such as spectral bands, vegetation indices, and textural images as extra bands	(e.g. Lu 2005; Lu et al. 2012)
Active sensor data	Radar	Backscattering coefficients, textural images, interferometry SAR, and Polarimetric SAR interferometry can be used as variables	(e.g. Mitchard et al. 2011; Nafiseh et al. 2011; Saatchi et al. 2011b; Carreiras et al. 2012; Sarker et al.2012)
	Lidar	Lidar metrics based on statistical measures of point clouds or estimated products (e.g. CHM or individual trees) can be used as variables	(e.g. Popescu et al. 2011; Nelson et al.2012; Chen 2013; Skowronski et al.2014)
	Combination of radar and lidar data	For mapping biomass over large areas where field plots are scarce, lidar samples (e.g. strips) can be taken. Lidar-derived biomass calibrated by field data is then used as dependent variable, and radar data are used as independent variables for developing biomass estimation models. Lidar-derived biomass serves as "virtual" field data to create a spatially representative biomass "truth" dataset for mapping biomass wall-to-wall using radar data.	(e.g. Sun et al. 2011; Tsui et al. 2013)
Integration of optical and/or active sensor data	Fusion of different sensor data e.g. optical and radar data	Fusion of Landsat and radar data to generate an enhanced multispectral image using different techniques such as wavelet-merging.	(e.g. Chen 2013; Montesano et al.2013)
	Combination of optical and radar or lidar as extra variables	Lidar and/or radar data are combined with optical-sensor multispectral bands as extra variables	(e.g. Nelson et al. 2009; Chen et al.2012; Selkowitz et al. 2012; Pflugmacher et al. 2014; Vaglio Laurin et al. 2014)

Table 2: Potential variables used in a biomass estimation procedure (adapted from Lu et al. 2014)

Optical sensor data are commonly used for biomass estimation; they can produce data at various spatial, spectral, radiometric, and temporal resolutions that are suitable in extracting variables for biomass estimation. Many techniques, such as vegetation indices, image transformation algorithms (e.g. principal component analysis, PCA; minimum noise fraction transform; and tasselled cap transform, TCT), texture measures, and spectral mixture analysis (SMA), have been used to produce new variables from optical multispectral data (Lu 2006).

The methods are based on spectral responses (spectral bands or vegetation indices and transformed images) (Bannari et al. 1995; McDonald et al. 1998 Foody et al. 2003; Zheng et al.2004), textural images (e.g. the gray level co-occurrence matrix (GLCM)-based texture measures) (Lu and Batistella 2005; Kuplich et al. 2005; Kayitakire et al. 2006; De Grandi et al. 2009; Sarker et al. 2012) or the combination of both (Lu 2005; Lu et al. 2012).

Several studies establish that methods based on spectral responses perform better when the forest stand structure is relatively simple (Lu et al. 2004; Lu 2005), while the textural images are more important in complex forest stand structures. The combination of the two methods improved biomass estimation compared to the use of individual spectral responses or textural images alone (Lu 2005).

Limitations in the application of optical sensors are related to saturation problems for forest sites with high biomass density and the influence of external factors such as atmosphere, soil moisture, vegetation phenology, and growth vigor spectral-based variables. They are suitable for the retrieval of horizontal vegetation structures such as vegetation types and canopy cover, but not for estimation of

critical parameters for biomass estimation such as tree and canopy height. Some optical sensor data such as ALOS/PRISM, Terra ASTER, and SPOT provide a stereo-viewing capability that can be used to develop vegetation canopy height, thus improving biomass estimation performance (St-Onge et al. 2008; Ni et al. 2014).

Long wavelength radar data are an important data sources for biomass estimation, especially when optical sensor data are not available due to the cloud cover in tropical regions.

Synthetic aperture radar (SAR) is a promising approach for studying forest biomass because of its ability in penetrating forest canopy to a certain depth, its sensitivity to water content in vegetation, and weather independency (Le Toan et al. 1992, 2011; Dobson et al. 1995; Kasischke et al. 1997; Huang and Chen 2013). The regression technique based on backscattering amplitudes (Santos et al. 2002; Sandberg et al. 2011; Rahman and Sumantyo 2013) and the interferometry technique based on backscattering amplitudes and phases (Balzter et al. 2007) are commonly used in biomass estimation (Lu et al., 2014). Because of the high correlation between vegetation canopy height and biomass, InSAR capability in providing vegetation height feature provides a promising tool for large-scale biomass estimation. This is especially important for tropical and subtropical regions because of the cloud-cover issue (Kellndorfer et al. 2004; Solberg et al. 2014).

The Polarimetric SAR interferometry (Pol-InSAR), a combined polarization and interferometry, is a recently developed radar remote sensing technology. Pol-InSAR produces more sensitive characteristics in spatiality as well as in shape and direction than interferometry or polarimetry for forest diffusions (Lu, et al., 2014). A

common biomass estimation procedure is primarily to estimate forest height using coherence information (Cloude and Papathanassiou 2003) and then convert it to biomass through correlation analysis (Garestier and Le Toan 2010).

The major limitations are connected to the possibility of distinguishing vegetation types (Li et al. 2012) and to the noise and outliers in the data, thus resulting in difficulty in biomass estimation. Nevertheless, these techniques are attracting increasing interest considering the referred capacity in penetrating complex forests structures, the high correlation between vegetation canopy height and biomass and weather independency.

Data saturation in optical and radar data is an important factor influencing the accuracy of biomass estimation in forests with complex stand structures, on the contrary lidar is capable to extract canopy height information even at high levels (>1000 Mg ha^{-1}; e.g. Means et al. 1999).

Because of the capability of lidar in providing both horizontal and vertical information of the canopy structures, its use leads to better biomass estimation performance than individual optical or radar data (Clark et al. 2011). In airborne lidar data, metrics can be extracted on the basis of either individual trees or areas (Chen 2013; Barbati et al, 2009; Corona and Fattorini 2008). The individual tree-based approach requires identifying tree features such as treetop (e.g. Popescu et al. 2002; Chen et al. 2006), crown radius (e.g. Popescu et al. 2003), or crown boundary (e.g. Chen et al. 2006; Zhen et al. 2014). Mapping individual trees requires high lidar data point density (generally 10 points per m2 or higher) and is

challenging in closed and multilayer canopies such as tropical rainforests (Lu e t al., 2014).

The area-based approach, which generates statistical metrics from laser returns or canopy height model (CHM) constructed from the returns, has been widely used (e.g. Lim et al. 2003; Chen et al. 2012; Lu et al. 2012; Chirici et al. 2016).

In the past, airborne lidar data were mainly applied in small areas due to high costs and large volume. As technologies advance, the use of airborne lidar data for biomass mapping will expand from local to regional levels (e.g. Skowronski and Lister 2012). For regional- to global-scale applications, spaceborne lidar – ICESat GLAS – was available between 2003 and 2009, and the use of GLAS data for biomass estimation has been shown to be valuable (Lefsky et al. 2005; Simard et al. 2008; Nelson 2010; Miller et al. 2011; Popescu et al. 2011; García et al. 2012).

The combination of airborne lidar and satellite imagery is another promising approach for large-area biomass mapping. Optical sensors, radar, and lidar each have pros and con and proper integration of them can improve biomass estimation accuracy (Walker et al. 2007; Kellndorfer et al. 2010).

Optical sensor data mainly represent land cover surface features, and radar data, especially with long wavelengths, can penetrate forest canopies to a certain depth capturing information about stems, branches, and understories. This providing more vertical stand structure information for vegetation types (Lu at al., 2014).

Lidar data are powerful for estimating canopy structure but has limited spectral information because laser point intensity is from one wavelength. Optical sensors

provide rich spectral information but the spectral reflectance does not have a strong relationship with canopy structure. Thus, lidar and optical sensor data are highly complementary. However, earlier studies that integrated lidar with optical data have reported mixed results. Some studies have shown that the addition of optical to lidar data registered only slight or no improvement in biomass estimation (e.g. Hyde et al. 2006; Clark et al. 2011; Latifi et al. 2012). Conversely, Anderson et al. (2008) and Vaglio Laurin et al. (2014) found that integration of lidar and hyperspectral data significantly improved biomass estimation.

The extent and complexity of a study area are the conditioning elements in the selection of suitable remote sensing data and biomass estimation algorithms. Thus, the integration of the proprieties of the different remote sensing data sources allows sufficient flexibility to cover different scales and conditions. Multiscale data from high spatial resolution datasets, such as QuickBird and lidar, medium spatial resolution datasets, such as Landsat and radar, and coarse spatial resolution datasets, such as MODIS, can improve the biomass estimation over the most diverse environments (Lu et al. 2014).

Biomass estimation at continental and global scales has gained increasing attention in the last decade due to the concerns over global climate change and daily availability of coarse spatial resolution images from MODIS and AVHRR (Hame et al. 1997; Baccini et al. 2008; Du et al. 2014)

Medium spatial resolution images such as Landsat are a common data source for biomass or forest attributes estimation on a regional scale (Chirici et al., 2008; Maselli et al., 2005). Previous research has indicated that spectral, spatial, and

subpixel fractional features are important variables for biomass estimation. In particular, integration of spectral and textural images provides more accurate biomass estimates than either dataset alone (Lu 2005).

On a local scale, biomass estimation results are typically used as reference data for validation or evaluation of other estimates from relatively coarse spatial resolution images. Therefore, local biomass estimations must be highly accurate and spatially precise. Optical sensor data such as QuickBird and IKONOS are common sources for this purpose (Thenkabail et al. 2004; Leboeuf et al. 2007). However, complex forest stand structures, tall tree-induced shadow problems, and high spectral variation in the same vegetation types reduce estimation accuracy. Use of textural images or object-based methods has the potential of solving these problems (Kayitakire et al. 2006). Nevertheless, use of the spectral and/or spatial information for biomass estimation modeling is often insufficient for obtaining accurate biomass estimates. Substantial research has indicated that at this scale, lidar-based biomass estimation can lead to better performance than optical sensor-based approaches (e.g. Zhao et al. 2009; Chen et al. 2012; Næsset et al. 2013; Tian et al. 2012).

At the finest scale is required single tree related information for more precise estimation of biophysical parameters, forest management and environmental planning. Single tree extraction has been commonly exploited in the field of forestry to reduce the manpower and cost needs in the traditional forest inventories. This is generally obtained by the usage of Airborne Laser Scanner (ALS) data by applying different algorithms for the extraction of pattern of single tree crowns (Gupta et al., 2010; Vauhkonen, et al., 2009; Hyyppä and Inkinen 1999; Persson, et al., 2002;

Koch, B et al., 2006; Morsdorf et al., 2004; Steinmann et al. 2012) or by high resolution multispectral or hyperspectral airborne Digital Data (Katoh, et al., 2012).

Techniques for tree-crown delineation are often based on first finding local maxima and then locating crown edges. A fundamental assumption inherent to crown delineation methods is that the main part of a crown is brighter than the lower edge of the crown, particularly at the boundary between crowns. Tree counting, tree-crown delineation, species identification, crown density estimation and forest stand polygon delineation have been made possible with high-resolution data such as that collected via the airborne Multi-detector Electro-optical Imaging Sensor (MEIS), the Compact Airborne Spectrographic Imager (CASI) and the Leica Airborne Digital Sensor (ADS),(Katoh, et al., 2012).

Biomass estimation exclusively from airborne visible imageries is not commonly reported in literature. The development of forest inventory has focused on high resolution images and especially on digital airborne measurements for forest survey and management (Leckie, 1990; Dralle and Rudemo, 1996). Several studies are reported about computerization and the analysis of digital aerial photographs for a determination of forest attributes (Greer, 1993; Holopainen and Lukkarinen, 1994; Blackburn and Milton, 1997; Tuomineen and Haapanen 2011; Uuttera et al., 1998). However, these studies are mainly based on CIR digital aerial imagery (containing near-infrared, red and green bands) that enhances the vegetation spectral contrast. The limitations and constraints occurring from the absence of NIR, SAR or LIDAR signals in the extraction of suitable variables for AGB estimation are the main

obstacles. These constraints are increased with the structural complexity of the stands.

Nevertheless, the sahelian xerophytic woodlands are characterized by simple structure and non-contiguous canopy cover with reduced vertical variation, compared to crown variability. Under these conditions, the capabilities of the lidar in capturing the vertical variability of the stands is not essential as they occur in other environments. Here, as observed in the data collected during the CV-NFI, a key variable associated with the AGB is the crown size and its horizontal projection that can be retrieved by optical sensors. Studies using very high spatial resolution satellite or airborne imagery have demonstrated that it is possible to accurately delineate single tree crown areas (Ke and Quackenbush 2011a and 2011b) in arid (Gärtner et al., 2014) or urban (Ardila et al., 2012) environments. Additionally several studies are reported on monitoring of vegetation status, phenology and variability of canopy structural parameters, based on ground visible digital imagery (Migliavacca et al. 2011; Vanamburg et al., 2006).

This left open the possibility of more investigation beyond the correlation between the vegetation cover and the visible signatures in order to retrieve variables for biomass estimation at least in the simple forest, like the one proposed in this study.

Considering the general availability of visible high spatial resolution, aerial imagery at low or no cost, and the speed, with which the data can be collected and processed, the investigation on the potential and limitations of these sources deserves some attention where simple and fast methods are required. Under these conditions, the opportunity to improve the biomass estimation, with an easily

accessible dataset can be considered an alternative or complement to ground-based methods, LiDAR and multispectral and hyperspectral satellite data remote sensing.

Traditional regression analysis is a method commonly utilized in developing biomass estimation models with remote sensing data. Parametric algorithms assume that the relationships between dependent (i.e. biomass) and independent (derived from remote sensing data) variables have explicit model structures that can be specified a priori by parameters. However, the relationships between biomass and remote sensing variables are often too complex to be captured by parametric algorithms. The biomass is usually nonlinearly related to remote sensing variables, and therefore, nonlinear models such as power models (Næsset et al. 2011; Chen et al. 2012) and logistic regression models (McRoberts et al. 2013) were often used to estimate biomass.

Nonparametric data-driven algorithms (often called machine-learning algorithms) have become popular in biomass modeling as they may provide more accurate estimates than linear regression models, especially when multisource data are used in large study areas. However, the model structure derived from these algorithms is often difficult to interpret (e.g. ANN). In other words, despite these algorithms possibly exceling in 'mapping' biomass, they do not help the 'understanding' of biomass estimation (Lu et al., 2014).

On the other hand, most biomass estimation models are only suitable for the specific study areas in which the models are developed and they are not transferable due to the effects of biophysical environments on remote sensing data.

The present study defines a simple and easily understandable method that can permit easy applicability and interpretation of the relation between observed variables and AGB. Moreover, it is expected that the developed model can be generally applied in other stands with similar characteristic, so the transferability is an essential element to consider. These peculiarities are essentials for the practical application, by the national entities, in the environment in which it is developed.

This is the reason to focus on a parametric linear approach that assumes the relationship between biomass as dependent variable and CPA as independent variable, investigating the most suitable scheme for its extraction from remote sensing data.

The fact that the AGB is calculated as a function of the crown projected area makes this method universally applicable in woodlands with similar characteristics being the only constraints the availability of proper imagery and allometric equations. As a consequence, the proposed method is easily explicable and its practical use, clearly understandable by users.

Resuming, the objective of this investigation is to assess the performance of single tree and area based approaches for AGB estimation, using high spatial resolution aerial visible color imagery over Cape Verdean xerophytics woodlands.

The hypothesis is that by analysis and processing of the image it is possible to classify and extract the tree crowns and calculate the biomass at tree and area level, using the available allometric equations and the defined models.

2. MATERIALS

2.1 STUDY AREA

Figure 1: Localization of Cape Verde

Cape Verde is an archipelago of ten islands (nine inhabited) and five islets located in the eastern Atlantic Ocean, approximately 570 kilometres (km) from the coast of Senegal, West Africa (16N, 24W) (Figure 1).

These islands occur in two groups, the Barlavento (in the north) and Sotavento (in the south). Total land area for the archipelago is 4,564 km^2.The archipelago is volcanic in origin, and is situated in the southwestern portion of the Senegalese continental shelf, on the oceanic crust.

The landscape is rugged on the younger islands (Fogo, Santo Antão, Santiago, and São Nicolau), with peaks reaching over 2,000m (highest mountain is Mount Fogo,

2,829 m), but relatively flat on the older islands (Maio, Sal, and Boa Vista). The degree of topographical variation is mainly related to the age of the islands and the presence of volcanoes. The major rocks are basalt and limestone, and there are deposits of salt and kaolin.

Cape Verde is on the edge of the North African arid climatic zone and has been heavily influenced throughout the last decade by the Sahelian drought. The climate is dry tropical with a strong oceanic influence that temperate thermal fluctuations. The dry season runs from December to July and the warm and wet season runs between August and November. Temperatures range between 20°C and 35°C, and average between 25°C and 29°C. Rainfall is irregular with great variability inter and intra annual, periodically the islands experience prolonged droughts. The torrential character of the rains cause heavy soil erosion and reduced water infiltration. Rainfall in most of the country ranges between 100 to 250 mm annually.

The climate is influenced by the cold current of the Canary Islands and three principal winds: the Northeast trade winds (80%), the South West monsoon (5%) and Harmattan from Est (6%) (Brochmann et al, 1997). The first is constant and blows from November to June. The second is hot and humid, irregular and unstable, blows between August and October and gives rise to rains. The third is dry wind that blows occasionally between October and June and carries large amounts of Saharan dust.

The combination of these winds with the orographic variability, locally influences the climate by creating a variety of microclimates.

The islands are divided into five climatic zones: Extremely arid (H1), dry (H2), semi-arid (H3), sub-humid (H4) and humid (H5) (Brochmann, et al, 1987).

Climate types H4 and H5 are on exposed slopes in the sector between N and E from the 500 meters altitude where the mists carried by trade winds determine a significant contribution in horizontal precipitation. In other sectors, the climate ranges from extremely arid to semi-arid, with the latter at higher elevations or in the watersheds.

Cape Verde's flora consists of 621 species of which 240 are indigenous and 84 endemic (Brochmann, et al., 1997).

The current vegetation is the result of significant human impact that led to the introduction of nearly two thirds of the current species and substantial changes in the ecosystem.

Much of the territory is covered by open or semi-desert herbaceous vegetation. Exotic species such as *Lantana camara* and *Furcraea foetida* become naturalized and invasive in the humid areas. Other areas are dominated by agriculture and forests of anthropic origin.

The original natural vegetation remains but in few areas of the country. In the past, it was likely represented by riparian formations of *Tamarix sp*. and *Ficus sycomorus* along the streams, by *Phoenix atlantica* dominating the sands dunes and savanna formations dominated by *Acacia albida* on the southern islands and local shrub formations dominated by *Nauplius daltonii*.

The rocky slopes were covered by *Sarcostemma daltoni*i and humid mountain slopes by continuous shrub vegetation with emerging trees of *Dracaena draco* and *Sideroxylon marmulano*. On semi-arid and sub-humid slopes *Periploca laevigata ssp. Chevalieri* occurred frequently.

In that period, it seems as if there never were true forests, as the indigenous tree species of *Dracaena draco, Sideroxylon marginata, Ficus sycamorus, Tamarix senegalensis, Acacia albida*, and *Phoenix atlantica* lack the ability to form continuous forest cover (Brochmann, et al., 1997).

The Cape Verdean forests are the result of afforestation programs created over past decades. The first afforestations, in order to minimize the adverse effects of ecosystem degradation, were initiated during the period of Portuguese colonization from 1930 with plantation of *Eucalyptus sp.* in the humid areas. Starting in 1950 onward, the introduction of new species such as *Pinus canariensis, P. radiata, P. halepensis, P. pinaster, Cupressus arizonica, C. sempervirens, C. lusitanica, Grevillea robusta, Eucalyptus camaldulensis, E. globosus, E. citriodora and E. gomphocephala* and *Kaya senegalensis* (Silva de Carvalho, 1994).

After the country's independence (1975) the afforestation was intensified (Table 3) in order to control the soil erosion, and increase the fuelwood and fodder availability.

During that period, the afforestation was concentred in the arid and semi-arid climatic zones introducing *Prosopis juliflora and Prosopis pallida, Parkinsonia aculeata* and numerous species of Acacia, among which *Acacia mollissima, A.cyanophilla, A. holosericea Acacia bivinosa, Acacia seleciana, Acacia Vitorie.*

18

Among these species, *Prosopis sp.*, for its ability to adapt to the soil and climate of cape Verdean islands, currently represents the 61% of wood species in terms of frequency throughout the country and 91% on Santiago Island (National Forestry Inventory 2012).

Period	Up to 1975		1976-1993		Total	
Island	Area (ha)	N° trees	Area (ha)	N° trees	Area (ha)	N° trees
S. Antão	432	324,000	5,049	2,401,262	5,481	2,725,262
S. Vicente			1,378	684,595	1,378	684,595
S. Nicolau	135	78,500	2,100	962,530	2,235	1,041,030
Sal			2	803	2	803
Boa Vista			3,180	1,238,724	3,180	1,238,724
Maio	500	75,000	2,404	785,464	2,904	860,464
Santiago	1,130	837,000	40,908	16,035,702	42,038	16,872,702
Fogo	725	500,000	8,943	4,262,077	9,668	4,762,077
Brava	37	15,000	1,966	914,699	2,003	929,699
tot	2,959	1,829,500	65,930	27,285,856	68,889	29,115,356

Table 3: Afforestation of cape Verdean islands (source *Direcção dos Serviços Florestais*)

The study area is located in the south sector of Santiago Island, coordinates upper left 15°0′33.368"N; 23°37′42.82"W – lower right 14°56′11.818"N; 23°27′40.946"W (Figure 2).

2.1.1 STUDY AREA CHARACTERIZATION

The study area covers a surface of 14399 ha in the arid and semi-arid climatic zones representatives of xerophytics woodlands of the island.

Approximately 44% of the land area is covered by forests, (Figure 2); the remaining non-forested land includes non-productive areas, agriculture and urban areas.
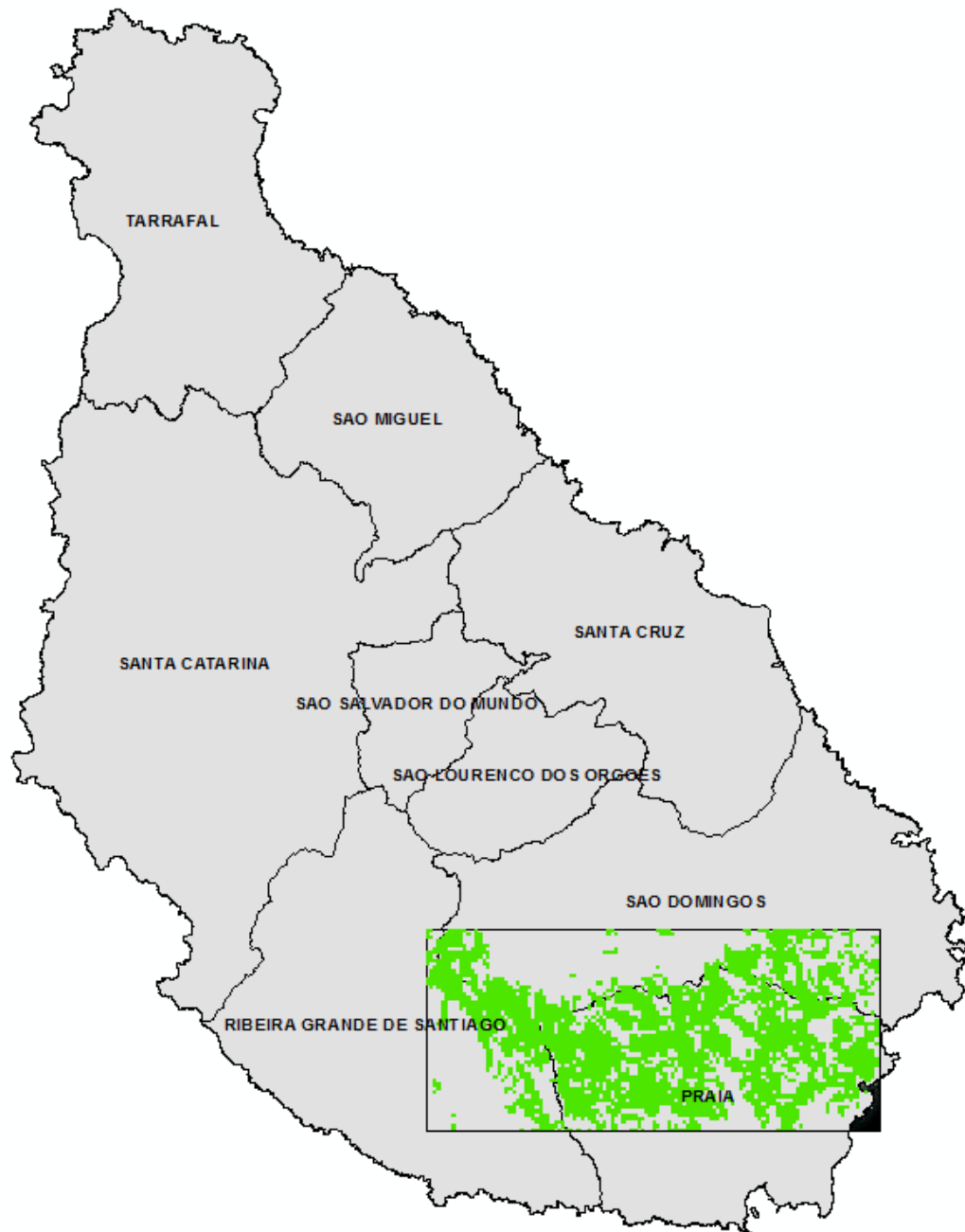
Figure 2: Localization of the study area in Santiago Island

Figure 3: Aspects of the woodlands that are object of this study

These woodlands are composed by shrub-like growing species (Figure 3), *Prosopis sp.* represents the 95% in frequency, of the total fifteen wood species observed. Other species with some noticeable participation are *Jatropha curcas*, *Acacia nilotica*, *Acacia Senegal*, *Parkinsonia aculeata and Acacia albida.* The average canopy cover is 43%, and the mean tree density is 252 trees ha^{-1}. The main dendrometric parameters describing the forest type in the study area, based in the field data (184 plots and 2218 trees), are reported are reported in table 4.

	Crown area , m^2	Tree Height, m	Tree Biomass, Kg	Mean AGB, Mg ha^{-1}
Mean	19.29	3.52	63.21	12.701
SD	12	1.19	58	8978
CV	64%	34%	92%	71%

Table 4: Mean, standard deviation and coefficient of variation of main dendrometrics parameters describing the forest type in the study area

Due to the adverse edaphoclimatic conditions and goat grazing, trees in the area are characterized by small dimensions, reduced crowns and low stature. When the local microclimate is more favorable, as in the streams and valleys protected from the winds, trees are bigger with denser canopies that can create continuous canopy cover. The soil is covered by grass only in the humid season (from August to November) and in the remaining months it is generally bare or covered by dried grass. These characteristic are favorable for tree crown extraction from images, since there is not overlap of canopies, the individuals can be easily detected and the bare soil is generally spectrally different and well defined from the crowns. On the other hand, the reduced crowns which are small and leafless, exhibit limited greenness and pose additional challenges to estimate correctly the sparsely existing biomass. The correct balance of these characteristics is essential in the image of processing to define an accurate method for tree crowns extraction and biomass calculation.

The data used as ground truth for the study are based on the fieldwork that was carried out during the first phase of the CV-NFI (2009) under the coordination of the author.

A forest non-forest map was created by manual delineation of high-resolution aerial orthophotography. During the first step, a grid of 150 m squares was overlapped to the image, and every square was classified according to the observed land cover. The minimum mapping area for each land cover class was defined at 5000m^2. Following this scheme, all the squares that presenting in their centre a forest cover of > 10 % with a minimum area of 5000m^2 were classified as forest and those with a forest cover >5% and <10% were classified as open forest. Only forest area is considered in the present study.
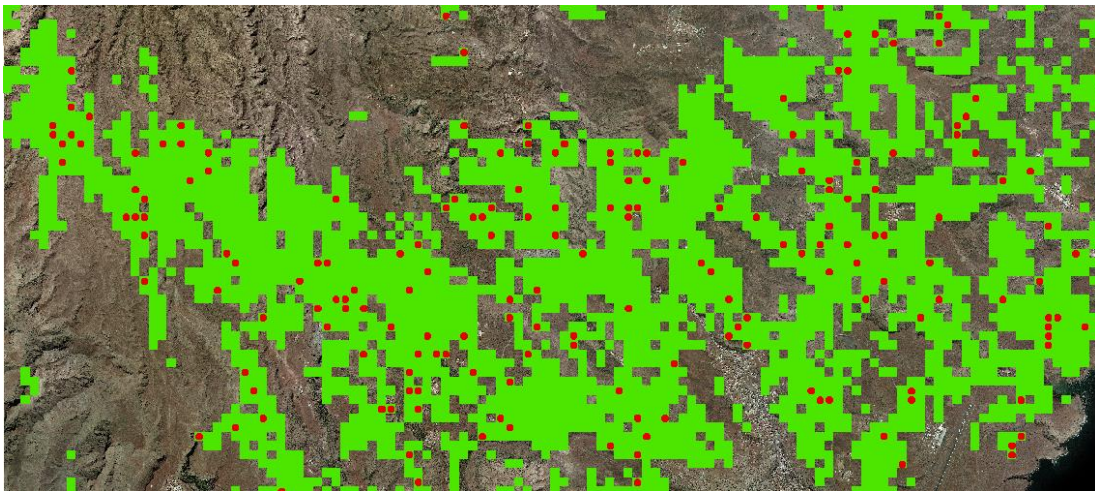
Figure 4: Detail of forest map and field plots in the study area.

A subset of the central points classified as forest was selected with a sampling intensity of 10% by means of simple random sampling without replacement

(SRSWOR) and surveyed in the field (figure 4). The plots were configured as circles of 500 m^2.

All trees in the plot with a height more than 50 cm were mapped and described.

The data collected are the following:

Tree base position, Tree species, Tree height (m), Crown projected area (based on 4 perpendiculars radius).

The field work was realized using the *Field Map* system. The system is composed of GNSS equipment (*GPS II SXBlue*), laser rangefinder/hypsometer *ForestPro* and electronic compass *MapStar Module II,* connected to a field computer with the field application (software *Field-Map Data Collector*). The location and navigation to the sample plots was conducted with the aid of GNSS equipment, connected to the field computer with a digital background map with the sampling plots. The position was recorded by averaging the GSSN position (at list 20 records) in open sky conditions and then completed by compass navigation until the center of the plot. Then all the trees were mapped and measured. Four pictures were taken, from the center to the four major directions (North, East, South and West) in each inventory plot. The data collected were directly stored in the database in the field computer.

Data processing was realized with *Field-Map Inventory Analyst* (FMIA) software in order to calculate the secondary variables such as crown width, canopy cover, aboveground biomass and the aggregation of the data from tree to plot level.

2.3 AERIAL PHOTOS

The imagery dataset used for this study is an aerial RGB orthophoto acquired in January 2010 with spatial resolution of 40cm (Table 5).

Radiometric & spectral resolution	Natural colour (RGB) 24-bit colour (3 x 8 bits per band) Red, blue, green
Horizontal accuracies	±3 pixels
Sensor information	Analogic camera
Image width, height (pixels)	100000 x 125000
Ground sample distance (GSD)	0.4x0.4 m
Sun angle	$>40^{o}$
Fly altitude	3800 m
Source	Geodata Air S.A.

Table 5: The characteristic of the imagery used in the study

The image was pre-processed by clipping the region of interest and converting from *.ecw to GeoTIFF format.

The Visible Atmospherically Resistant Index in the form VARI=(Green−Red)/(Green+Red−Blue) (Gitelson et al. 2002) was calculated at this step and used as an additional band in the image processing.

3. METHODS

3.1 AGB ESTIMATION USING IMAGERY DATA

The AGB was calculated at single tree level and area based. The following scheme was applied: (1) tree crown mapping, (2) Tree crown extraction and crown projected area (CPA) calculation, (3) tree height modeling (only for single tree approach), (4) biomass calculation.

The vector layer as forestry area, field plots and crowns polygons from field measurements were organized in a GIS for the following steps.

3.1.1 TREE CROWN MAPPING

Several techniques and algorithms were tested to define the best scheme for vegetation mapping.

The processes tested as follows:

1. Image segmentation followed by a supervised classification of the segments using the k-nearest neighbour, SVM, Decision and Random Trees classifiers.

2. Image segmentation and extraction of signatures from the segments. These segment-based training sites were used as input into pixel-based classifiers and were finally used for further classification by combining the pixel-based and the segment-based methods. Maximum Likelihood, Fisher and K - nearest neighbor classifiers were tested in this process.

3. Unsupervised classification using the ISOCLUST, ISODATA and KMEANS clustering techniques followed by a threshold segmentation/classification algorithm and multiresolution segmentation based on the region grow on object algorithm (Adams 1994), (Shih and Cheng 2005).

After a number of tests we decided to apply the process nr.3 described in detail below.

The first step performed was a classification of the image using the ISOCLUST algorithm. ISOCLUST is an iterative self-organizing, unsupervised classifier based on a concept similar to the well-known ISODATA routine of Ball and Hall (1965) and cluster routines such as the H-means and K-means procedures. On the basis of a histogram, indicating the frequency of pixels that belong to each seed cluster (figure 5), a decision was made to perform the classification on 8 cluster bases.
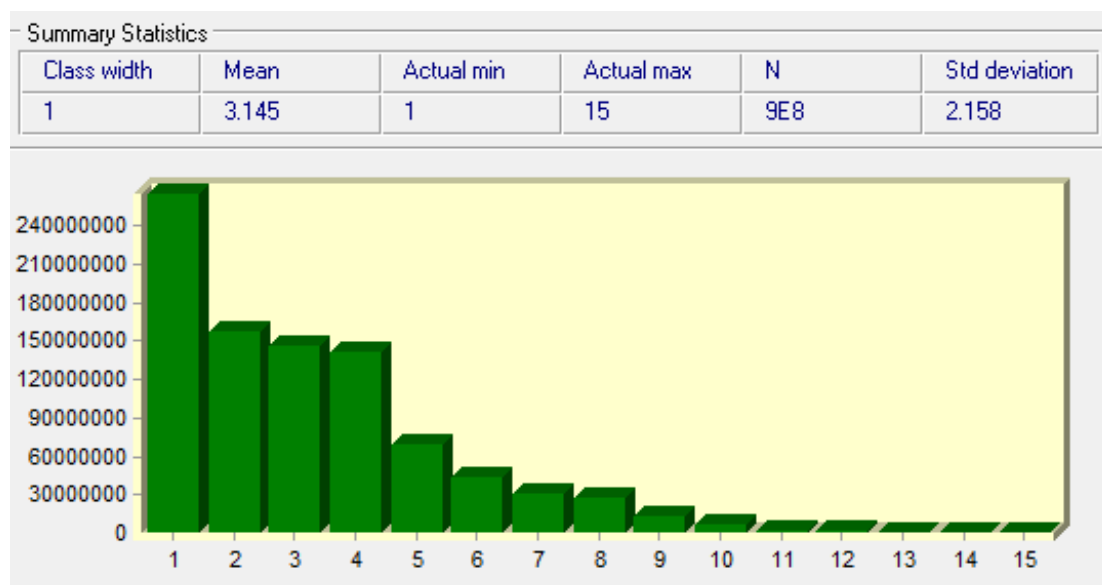
Figure 5: Histogram indicating the frequency of pixels that belong to each seed cluster

Figure 6: Result of ISOCLUST classification
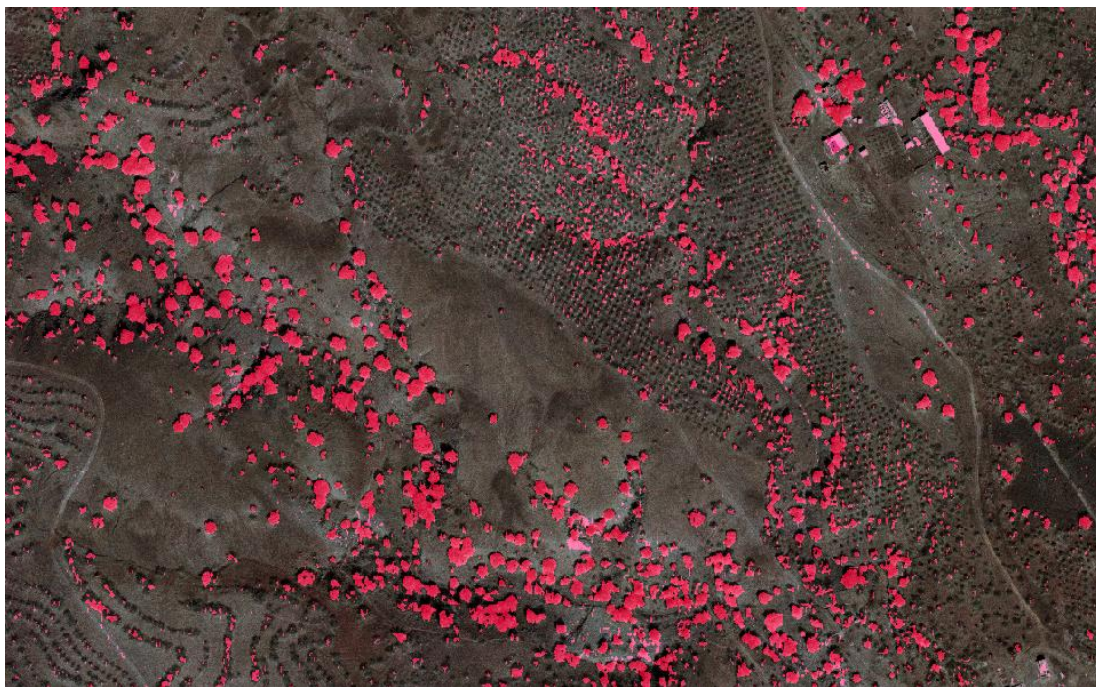
Figure 7: Tree canopy map obtained by VARI image processing

Following the classification, a visual analysis was performed in order to identify the

clusters representing the tree crowns and soil (figure 6).

The result of ISOCLUST classification permits an initial identification of clusters representing soil and trees but some clusters are mixed between soil and crowns, avoiding a correct extraction of the canopies for biomass calculation.

Complementary the analysis of the VARI image showed good results in separating the trees from the soil (figure 7). In this case, the soil is completely excluded and the big and green canopies perfectly identified. The problem in this case is posed by the smallest and leafless crowns that are lost.

With the purpose of cleaning and separating and the mixed clusters, a process of fusion and resampling of the two images was performed. On this basis, the ISOCLUST image was reclassified assigning negatives numbers to the clusters representing soil and high positives numbers to the ones representing the canopies. The mixed clusters, that include canopies portions, shadowed areas and bright parts of canopies and soil were reclassified to intermediary values (table 6).

Cluster Nr.	Description	Value assigned
Cluster 1	Bright side of crowns and soil	10
Cluster 2	Soil	-10
Cluster 3	Trees and some dark soil areas	20
Cluster 4	Soil	-10
Cluster 5	Scattered pixel of crowns	5
Cluster 6	Light soil	-10
Cluster 7	Trees and shadows	50
Cluster8	Scattered pixels of soil and crowns	3

Table 6: Description of the clusters resulting from the ISOCLUST classification and new values assigned by reclassification algorithm

This reclassified image was then fused with the VARI image. The fusion was realized by a sum between the two images. To amplify the difference between the negative numbers, representing the soil pixels, and positive numbers representing the tree pixels (figure 8), the VARI image was previously reclassified in the range -200 +200.

The resulting image was then reclassified to increase the difference between the soil and canopies pixels, for this, all the values between the minimum (-210) and -5 were reclassified to -10 and all the values >20 to 100. The process was followed by mean filtering with a 3 × 3 window followed by reclassification in equal intervals of 1-255. The accuracy of the result was assessed by visual interpretation over the scene on the basis of the RGB image (figure 9).
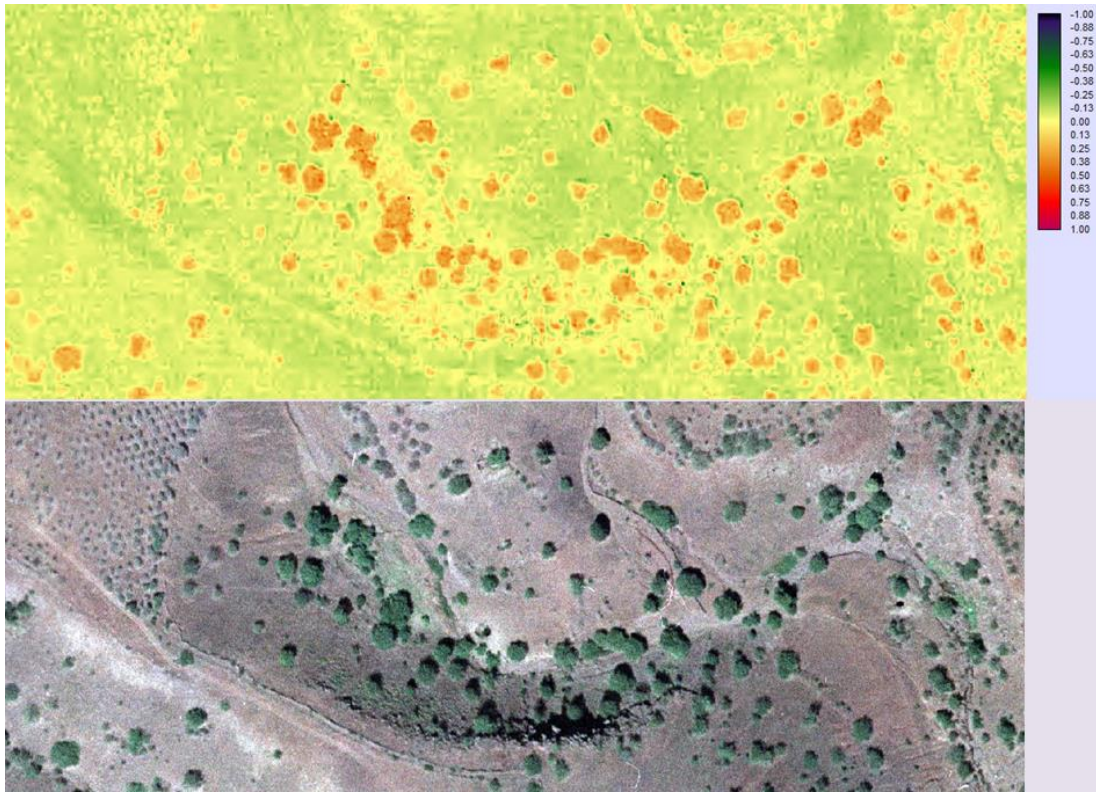
Figure 8: The VARI of a portion of the scene.
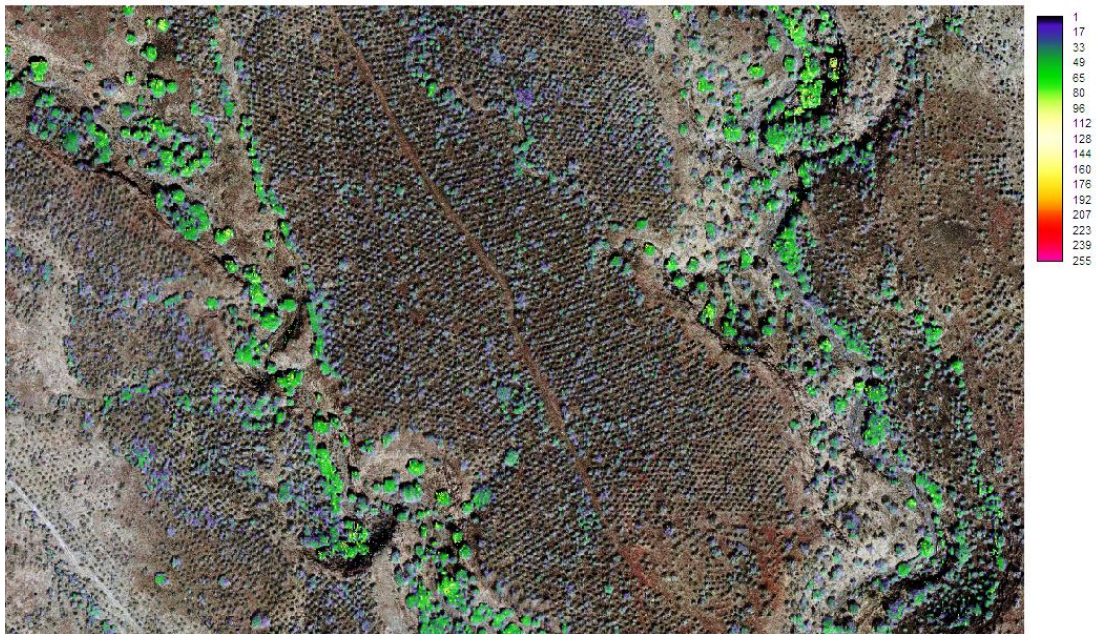
Figure 9: Overlap between the RGB and the ISOCLUST+VARI reclassified image for classification accuracy assessment

3.1.2 TREE CROWN EXTRACTION AND CPA CALCULATION
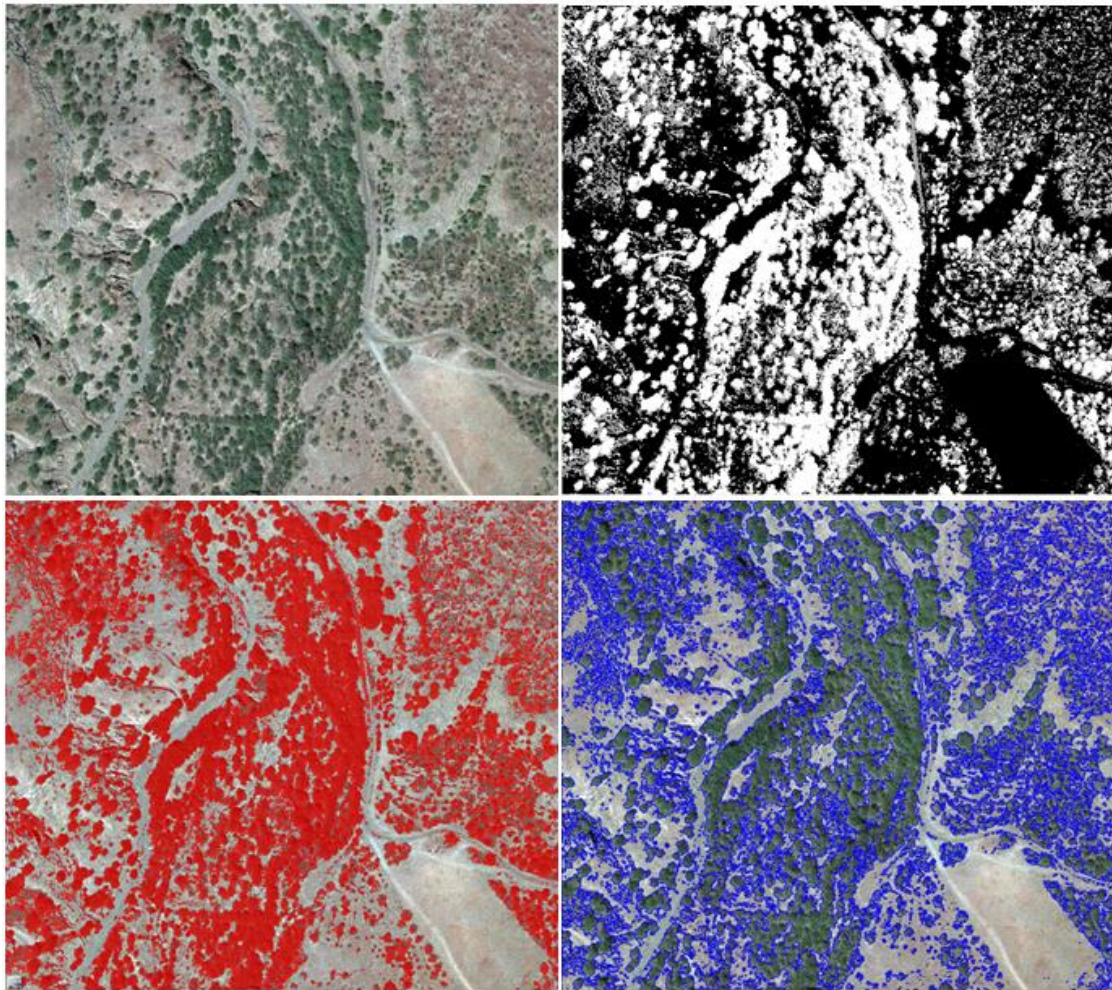
Figure 10: Sequential steps of image processing from the composite RGB image (a) to the ISOCLUST +VARI fusion (b) and threshold classification (c) and segmentation (d).

Two different approaches were followed: area based and single tree level.

Area Based:

The classified image was processed by reclassification to the values 0-1 (soil–tree respectively) with a sequence at different thresholds. The accuracy of crown

mapping was tuned by an iterative process. The first level was assessed by contrasting the crown map image with the RGB.

The image was then generalized, reducing the pixel size to 22.4m x22.4 m (equal to the field plot area of 500 m^2), using the pixel aggregation as the contraction rule. The total CPA per pixel was then calculated.

The final tuning of the model was realized by regression analysis between the true and image retrieved CPA. During this process a sequence of decreasing threshold levels was tested and the resulting Pearson correlation coefficient and Normalized Root Mean Square Error (NRMSE) was observed in order to define the optimal threshold level (table 7).

Threshold	NRMSE CPA	Coeff. of Det. % AGB	NRMSE biomass
15	59%	49.64%	59%
12	55%	51.41%	55%
10	51%	53.23%	51%
9	49%	54.28%	50%
7	46%	55.35%	48%
5	46%	55.35%	48%

Table 7: Variation of the R^2 and RMSE% at different thresholds

Single tree approach
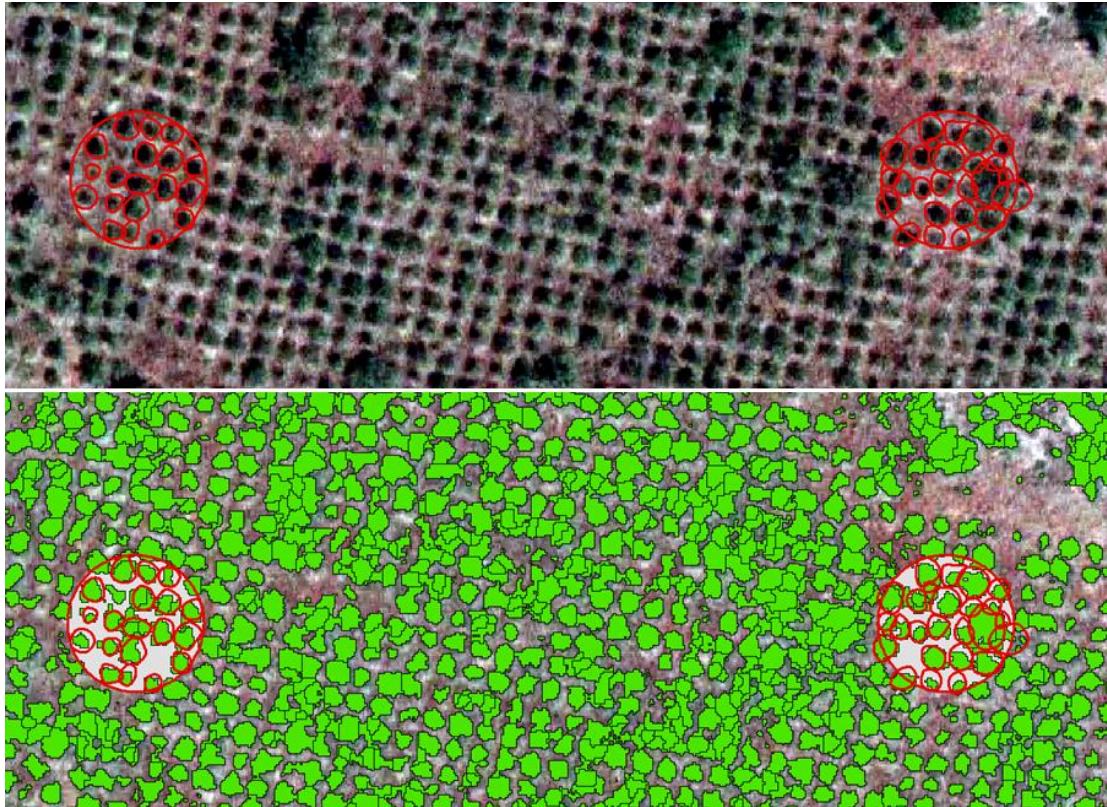
Figure 11: Comparison between field measured crowns (red polygons) and segments obtained by image processing (green polygons).

The image was processed by the threshold segmentation/classification algorithm (figure 10) followed by the subsequent step of multiresolution segmentation based on the region grow on object algorithm (figure 11).

Similar to the area based approach, the first step was to define the optimum threshold by testing a sequence of decreasing values.

At the next step, different combinations of the settings, such as the scale factor, color/shape, smoothness/compactness were iteratively tested (figure 12) in order

to define the best combination that minimizes the RMSE of the crown area and biomass estimation.
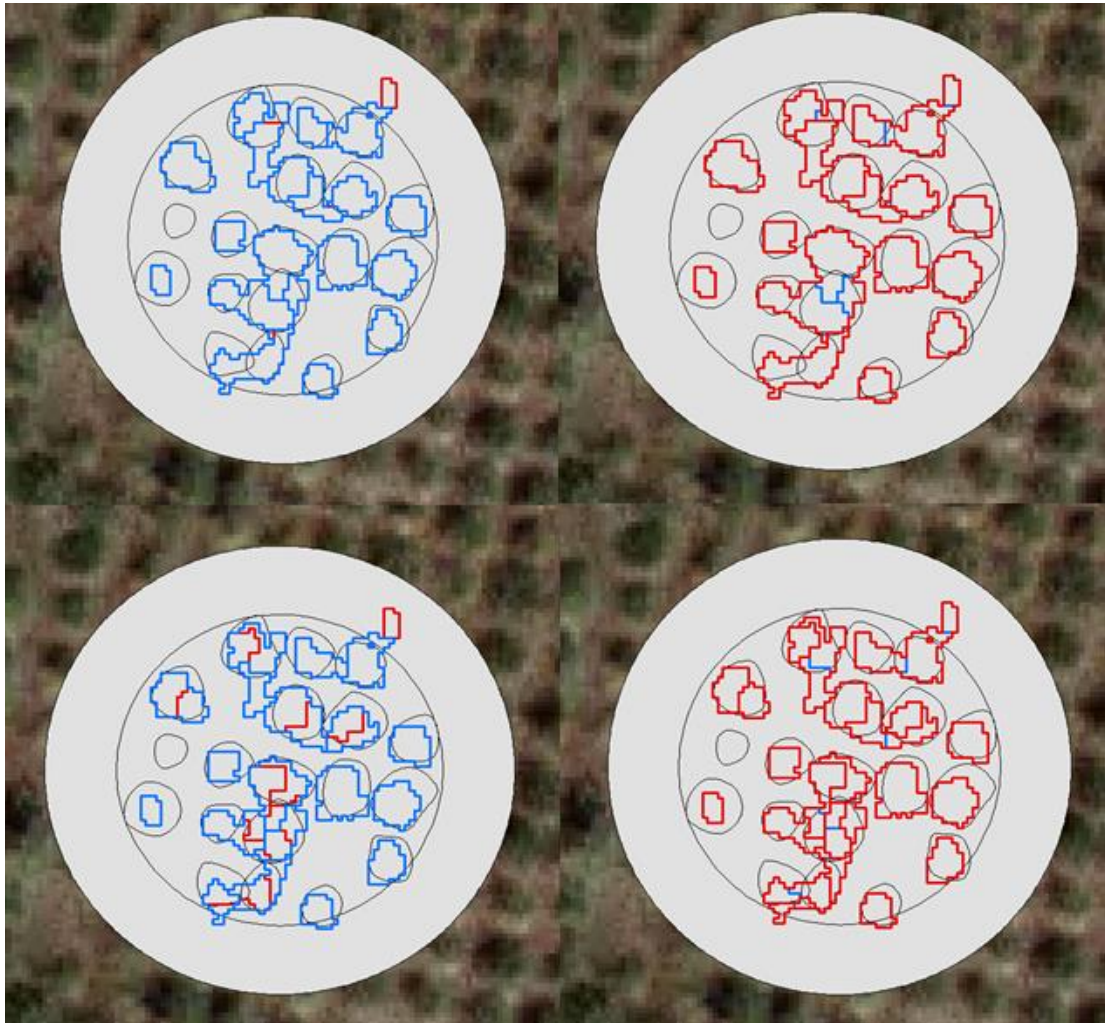
Figure 12: Comparison between different setting of color/shape and smoothness/compactness. The blue lines represent the results of higher compactness (1) and the red lines higher smoothness (0), the black lines represent the field plot and crowns. A) color/shape 0.5 smoothness/compactness 1; B) color/shape 0.5 smoothness/compactness 0; C) color/shape 1 smoothness/compactness 1; D color/shape 0 smooth-ness/compactness 0.

The objects were converted into vectors and processed by GIS software.

The following steps were: area calculation and selection of tree crown polygons corresponding to each field plot for model accuracy assessment. In order to minimize the edge effect, and simulate the same process of tree mapping in the

field, the selection of the polygons was performed using the spatial selection function *"target layers features have their centroid in the source layer feature"* where the target layers are the tree crowns polygons and the source layer are the field plots polygons.

3.1.3 TREE HEIGHT MODELLING

The tree height for each segment was calculated by the horizontal crown projection-height relation. The model was calculated on the basis of field data collected in 630 plots from Santiago Island for the Cape Verdean National Forest Inventory (CV-NFI) from *Prosopis sp.* (n=7171) (figure 13). The model is based on the equation:

$$\text{Tree height} = 1,2757 CPA^{0,3683} \quad (R^2 = 0.5331)$$
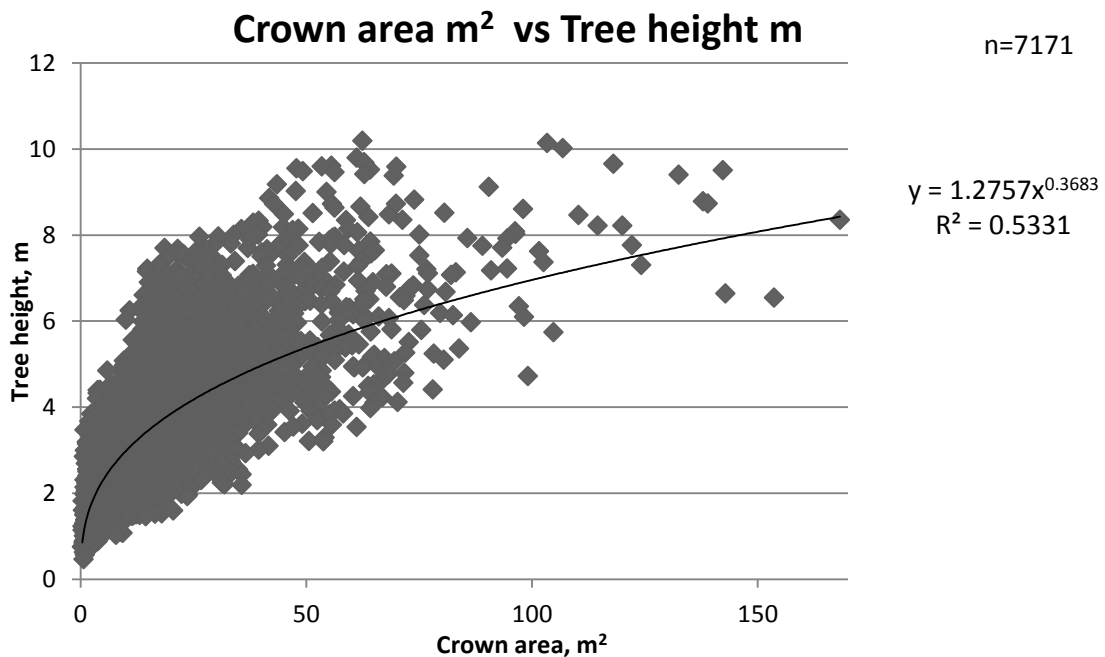
Figure 13: Relation between horizontal crown area and tree height for *Prosopis sp.* in Santiago island

3.1.4 BIOMASS CALCULATION

According to the approach as we tested, single tree and area based, the AGB was calculated in two different ways.

In the first approach and for the field data, the AGB was calculated by the allometric equations developed specifically within the CV-NFI (Cienciala et al. 2013). The study on biomass models used destructive sampling of *Prosopis juliflora* that was carried out on three islands, namely Santo Antão, Santiago and Maio.

The equation used is the one based on the crown width (CW) and tree height (Ht):

$$AGB = 1,098*EXP(-0,23+0,528*LN(Ht)+2,159*LN(CW)) \quad (n=237 \; r^2=0.729)$$

The biomass was calculated at single tree level, using as input variables the CPA, extracted from the images, and the modeled tree height. The biomass at plot level was then calculated as a sum of the individual AGB.

In the second approach, regression analysis, was used in deriving models for biomass as function of CPA. The AGB was calculated by the equation that minimizes the RMSE (figure14) using as input the total CPA of each 500m^2 pixels.
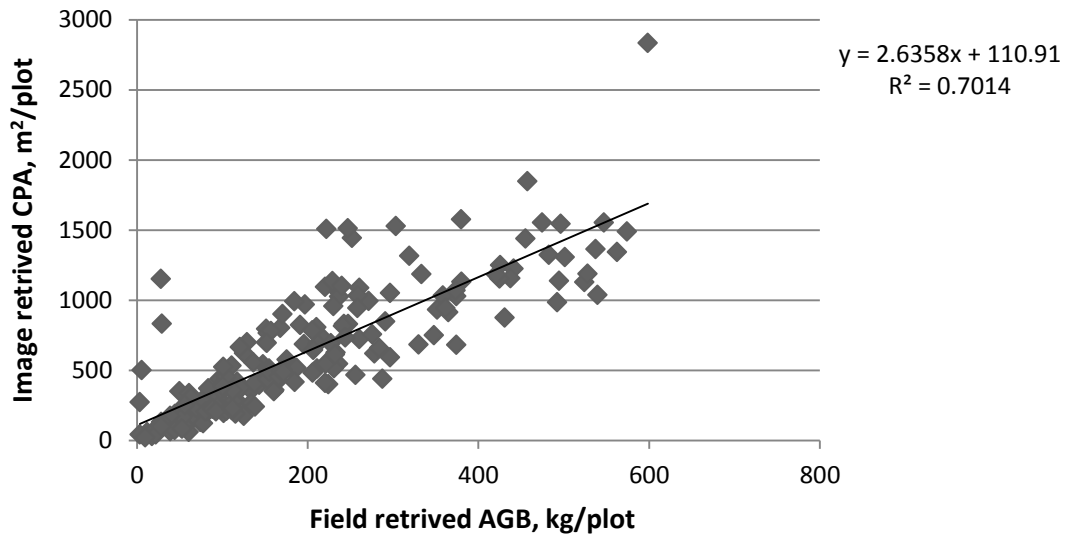
Figure 14: Relation between tree crown area and biomass.

3.2   ACCURACY ASSESSMENT

Biomass estimates and CPA measured from field plots were used as ground truth data to evaluate predictions of biomass obtained from the models.

The validation of AGB imagery estimation models was done against allometric-based (field-measured) biomass.

Traditionally, the accuracy of forest biomass/carbon estimates is assessed by calculating the root mean square error (RMSE) and the Pearson's correlation coefficient of the estimated and observed values (Congalton 2001; Congalton and Green 2009; Wang and Gertner 2013).

Accordingly, the accuracy of the values predicted was measured by RMSE (Equation 1) and the normalized root mean square error (NRMSE) to the mean of the observed data (Equation 2).

$$RMSE = \sqrt{\frac{\sum_{i=1}^{n}(X_{obs,i} - X_{model,i})^2}{n}}$$

Equation 1: RMSE

$$NRMSE = \frac{RMSE}{\overline{X_{obs}}}$$

Equation 2: NRMSE

The relationship between the different parameters was studied by linear and power correlations and the correspondent Pearson correlation coefficient and coefficient of determination (r^2).

4. RESULTS

4.1 TREE CROWNS MAPPING

The visual assessment of the classification accuracy shows good results all throughout the image (fig.15); good identification of the trees is reached even for the smallest crowns and in the most complex structures.
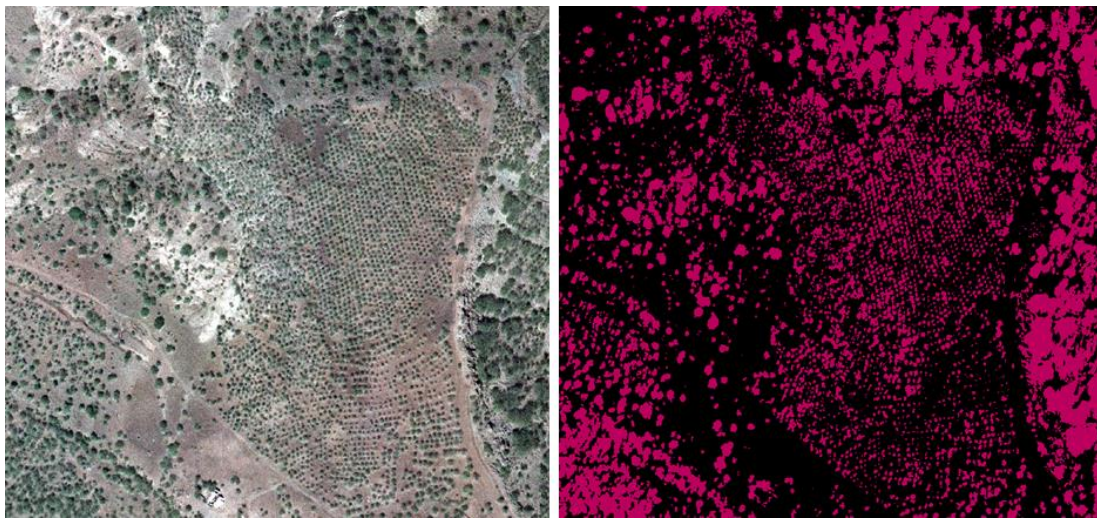
Figure 15: The final result of tree crowns mapping in a portion of the scene.

Only some localized and well identified areas, where the soil is darker or covered by grass, was impossible to completely separate the tree crowns from the background at the selected threshold. During image processing was observed that the use of higher threshold values can increase the accuracy in the shadowed and dark areas on the contrary lower threshold where better defining the tree crowns in the and the lighter parts of the scene. Obviously in the first case, the smallest trees and bright parts of the tree crowns are lost and in the second a quick increase in the noise and incorrect classification was observed. Increased results can be reached

working in sub datasets divided by more homogeneous characteristics of background and tree size and by using different thresholds for each condition.

4.2 MODELS TUNING

The tuning process performed in the image processing indicated that the primarily factor influencing AGB estimation accuracy is the classification of the image, followed by the scale applied in the image segmentation for the tree crown extraction in the single tree scheme. Threshold levels above seven resulted in a rapid increase of the RMSE whereas below five there was no change detected.

Little influence was observed in the fine tuning of color/shape and smoothness/compactness settings. In the tests performed a maximum of 2% of the total NRMSE of biomass estimation was affected by setting the color/shape and smoothness/compactness parameters to extremes values. The better results were observed in middle range of values reaching the minimum RMSE with the color/shape defined at 0.3 and smoothness/compactness at 0.6.

4.3 TREE CROWN PROJECTED AREA CALCULATION

The analysis of the data exhibits the possibility of an accurate calculation of the tree crown projections with a NRMSE of 40%. Analogous results are observed in the single tree and area based approaches at plot level and original resolution (figure 16 and 17a). The generalization at $500m^2$ pixels, applied in the area based approach, produces a decrease of the estimation accuracy. It seems due to the resampling

that enhances the edge effect when comparing the circular plots data samples with square pixels.
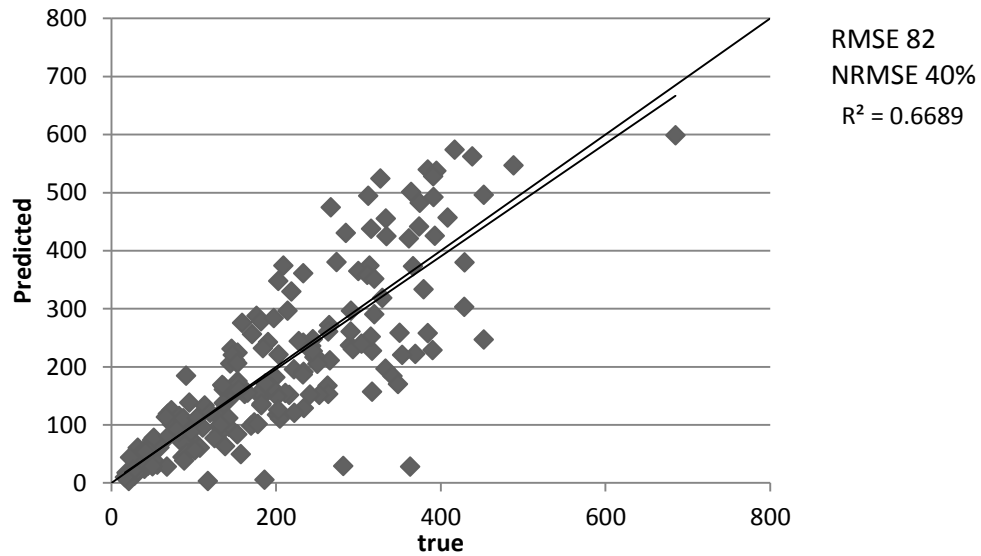
Figure 16: Relation between observed and predicted CPA, m^2 per plot ($500m^2$), in the single tree approach. The CPA is the sum of the individual's segments area having their centroid inside the plots

Figure 17: Relation between observed and predicted CPA, m^2 per plot ($500m^2$), in the area based approach. Figure A is the extracted CPA from the circular plots at original resolution. Figure B represents the CPA extracted from the spatialized map at $500m^2$ pixel resolution.

4.4 TREE DENSITY

The single tree approach assumes that each segment corresponds to an individual tree. On this base, the tree height of each segment is modelled and then the AGB is calculated. Nevertheless, in the segmentation of the image it is necessary to use a low scale that permits the mapping of the smallest trees that are widely present in the scene. As a consequence, the medium and big crowns are divided into multiple parts. The result is that the predicted number of trees is notably higher than the true value and the resulting RMSE is high and the correlation between the two values is weak (R^2=0.28) (figure 18).

RMSE 269
NRMSE 116%
$R^2 = 0.28$
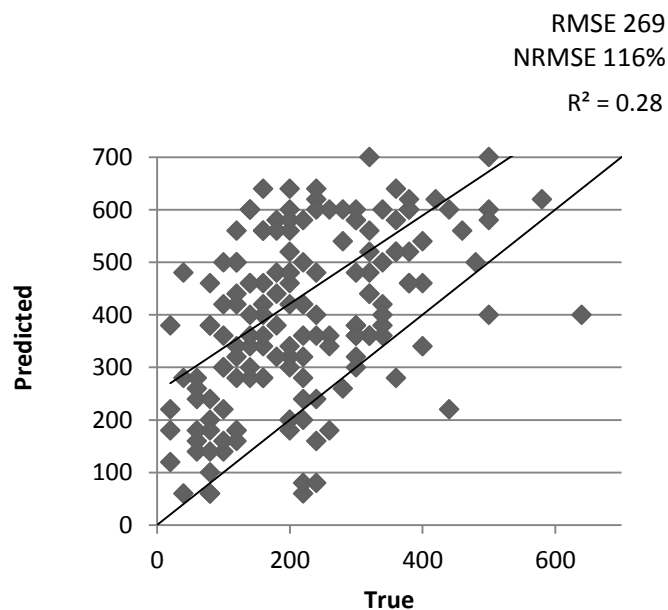
Figure 18: Relation between predicted and observed tree density nr ha^{-1}

4.5 BIOMASS CALCULATION

The biomass is estimated with similar values of NMRSE such as CPA, ranging from 39% to 55%. This suggests that the models used to estimate the AGB from the CPA

do not add relevant bias to the final results. The lowest RMSE is obtained by using the area based approach when the AGB is estimated from the circular plots at original resolution (Figure 20A). Similar results are obtained by the single tree approach when the biomass is calculated as the sum of all the segments having their centroid inside the plot (Figure 21A). In the first case, the performance is slightly better because the model is positively affected by the plots edges, where the field measured emerging canopies are defining the area of interest (fig. 19).

When extracting the attribute values, the feature definition image artificially contributes to the exact extraction of the edge pixels.

The RMSE increases (48%) when the biomass is modelled from the spatialized image at 500m^2 pixel resolutions. Nevertheless, this second scheme seems to be the correct one, considering the above observations.
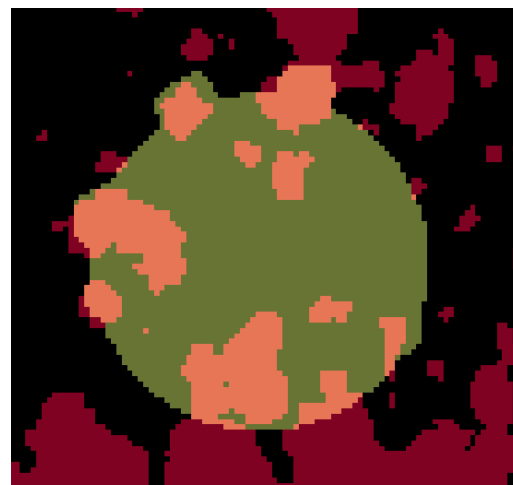
Figure 19: The edge effect in the area based approach (model) when the field plot with the emerging crowns shapes (green area) are used as feature definition image

In the single tree approach, the RMSE ranges from 42% to 55% (figure 21). In the first case, the ground truth AGB is contrasted with the sum of individual segments AGB having the centroid inside the corresponding plot. This should to be the correct scheme for the application of this approach. In the second case, the ground truth AGB, is compared with the AGB extracted from the spatialized map at 500m^2 pixel resolution.
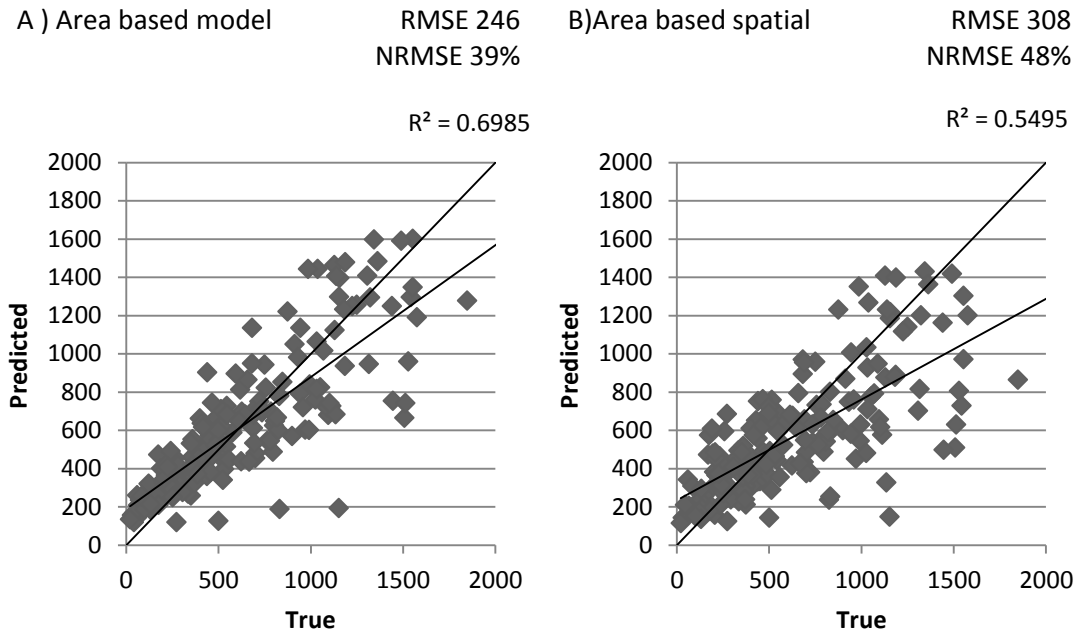
Figure 20: Relation between observed and predicted AGB, Kg per plot (500m^2), in the area based approach. The figure A is the estimated AGB from the circular plots at original resolution. Figure B represents the AGB extracted from the spatialized map at 500m^2 pixel resolution.
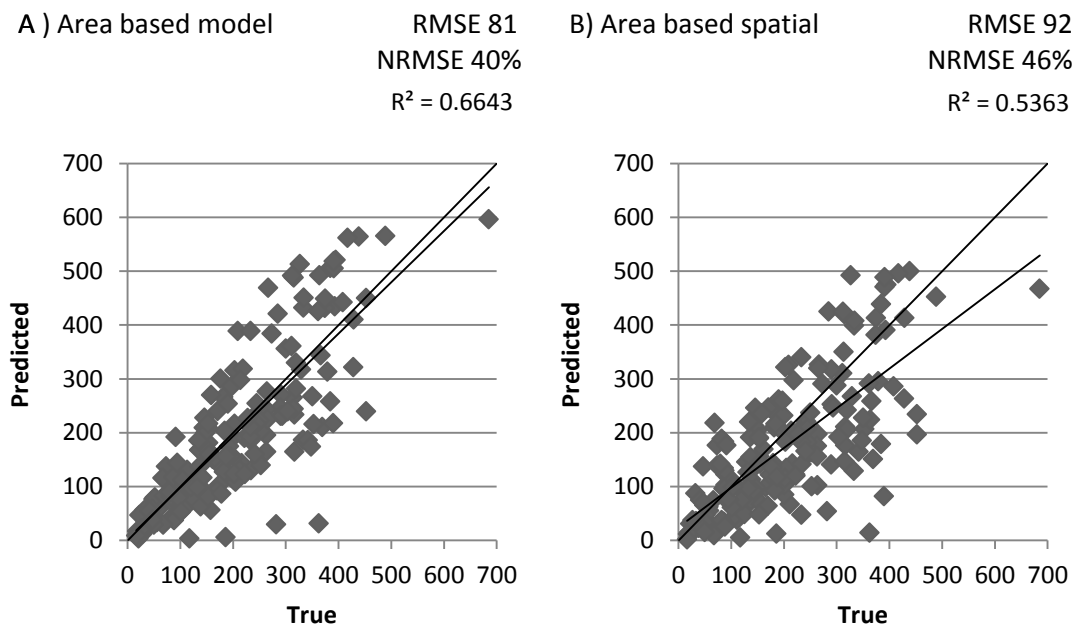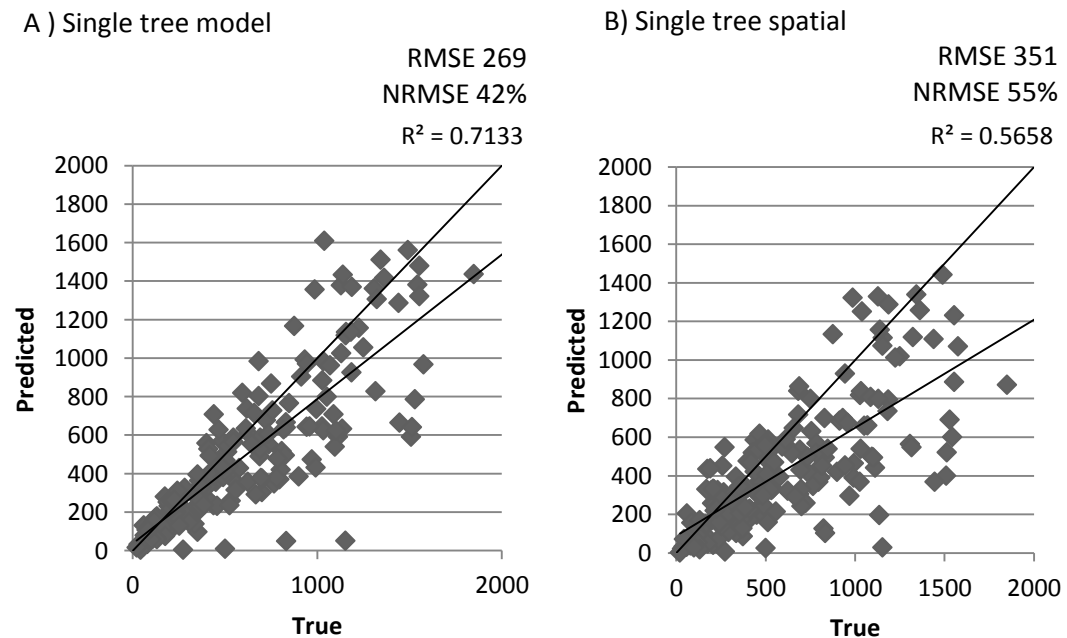

Figure 21: Relation between observed and predicted AGB, Kg per plot (500m^2), in the single tree approach. The figure A is the AGB calculated as sum of the individual's segments AGB having their centroid inside the plots. Figure B represents the AGB extracted from the spatialized map at 500m^2 pixel resolution.

In this case, a significant decrease of the model accuracy is observed when spatializing the AGB data to the new resolution.

It is necessary to consider that the single tree model simulates the same process of the field data collection. All the trees, with the base inside the plot, are measured and the crown portions following outside the plot area are accounted for the plot AGB estimation. When the single tree estimated AGB is spatialized to 500m^2 pixels, the biomass associated with each segment is proportionally attributed to the adjacent pixels. This reduces the predicted AGB for the reference plot introducing a bias in the comparison of the two values.
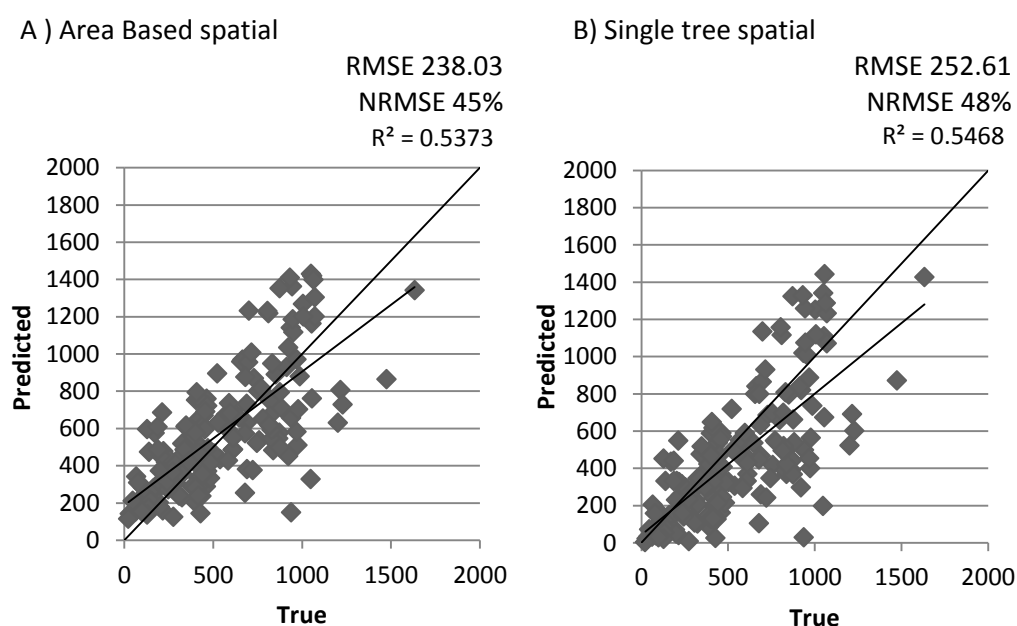
Figure 22 Relation between observed and predicted AGB, Kg per plot (500m^2) when the reference AGB is calculated using only the crowns portions falling inside the plots. In the figure A is contrasted with the AGB predicted by area based approach and in figure B with the single tree approach.

When the AGB extracted from the spatialized map at 500m2/pixel resolution is contrasted with a reference AGB, resulting only from the portions of tree crowns contained within the plot, the RMSE drop from 55% to 48% and from 48% to 45% in the single tree and area based approaches respectively (figure 22). This indicates that the bias due to the edge effect is stronger in the single tree model and an increase of the plot sizes can reduce the observed RMSE.

5. DISCUSSION AND CONCLUSIONS

The goal of this study was to evaluate the general applicability of models based on visible aerial imagery processing for single-tree and area based biomass estimation. The findings demonstrate that an accurate identification of trees crowns, horizontal crown area extraction and biomass estimation is possible in woodlands with the given characteristics.

The proposed method is based on the integration of clustering techniques combined with the Visible Atmospherically Resistant Index (VARI) and segmentation algorithms for tree crown extraction. This permitted the minimization of constraints due to poor spectral contrast between the background and tree crowns especially for brighter parts of the crowns and shadowed parts of the scene.

The prediction of single tree and plot AGB as a function of CPA as independent variables was both viable and accurate.

When observing the real distribution of biomass (figure 22), values between 0 and 750 kg/500m^2, the predicted values are similarly distributed to the observed ones. The mode is situated between 250 and 300 Kg both in the observed data and in the single tree predictions; it is slightly higher in the area based model.

On the other hand, at greater values, the two models tend to underestimate the biomass, this is more evident in the single tree approach.

A consistent group of points in the range between 1000 and 1500 kg is underestimated by the two models (figure 23 and 24).
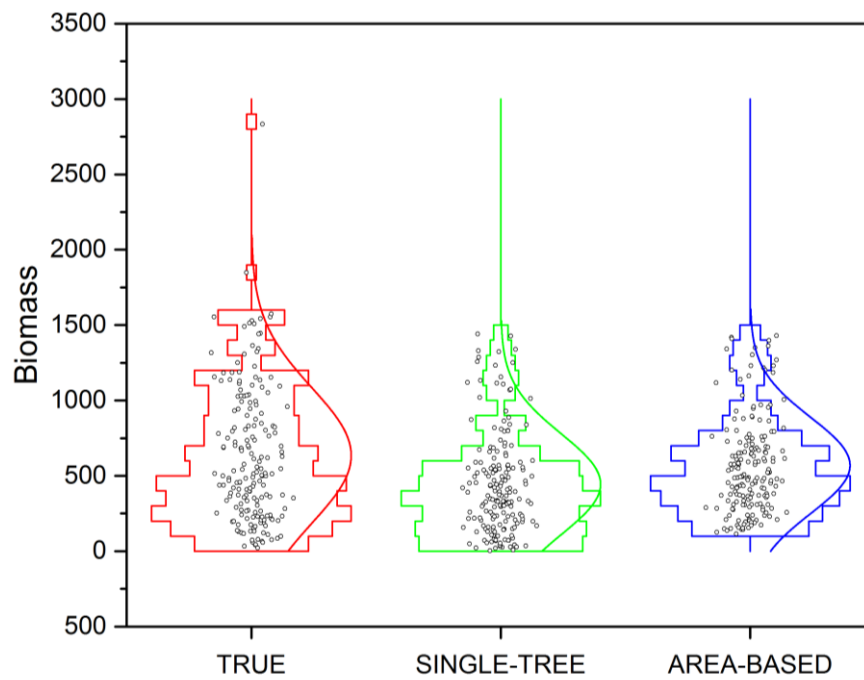
Figure 23: Distribution of the biomass observed and predicted by the two models.
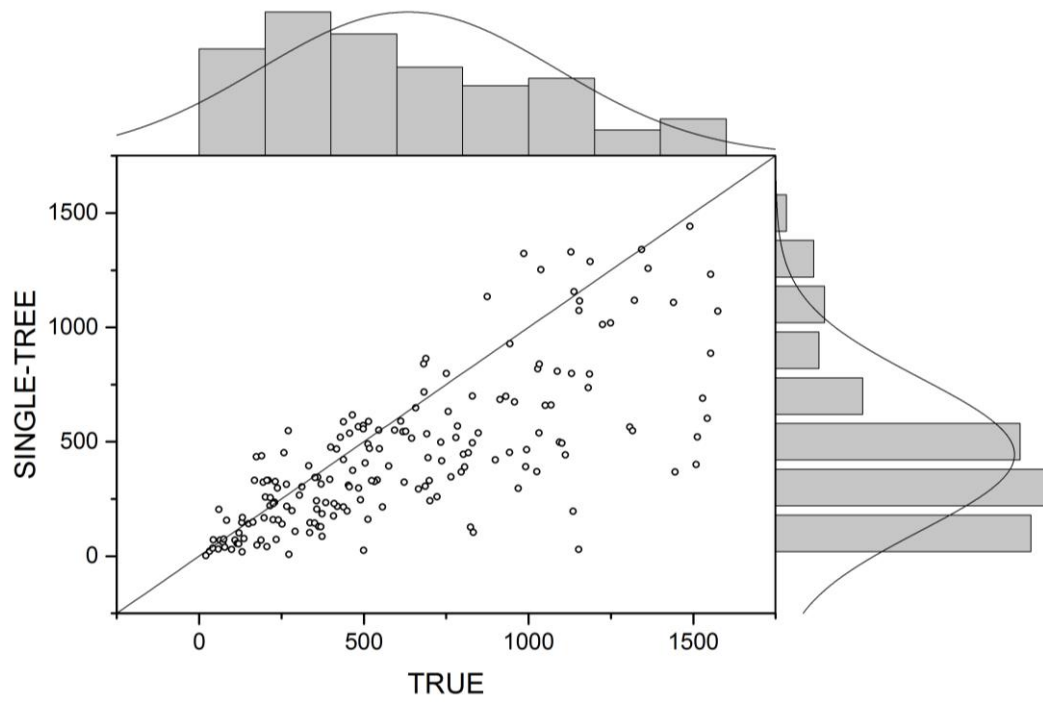
Figure 24: Distribution of the biomass in the single approach
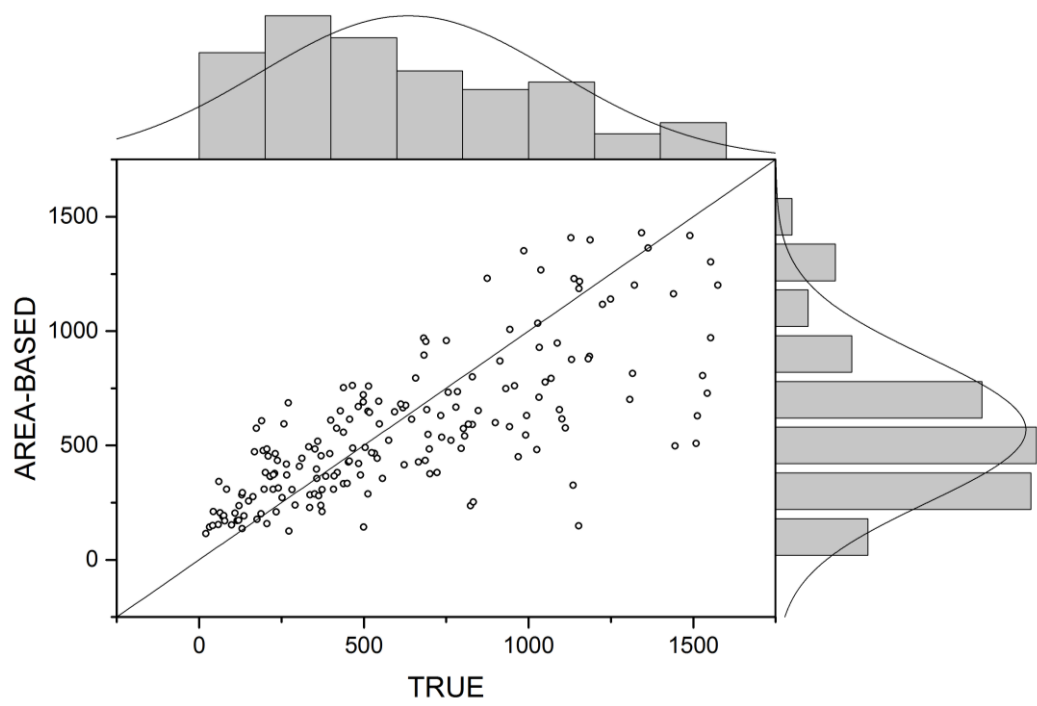
Figure 25: Distribution of the biomass in the area based approach

A possible explanation for this is that individual tree crowns are mapped basically on bases of the darker areas of the canopy and shadows. On the contrary, the brighter crown portions tend to be confused with the background. Therefore, in the crown extraction, part of the crown is lost and this is proportionally greater the bigger the tree is. This occurs because the tree height variation is considerably lower than the variation of the projected area of the crown. Moreover, in the sites with greater biomass, a partial overlap of tree crowns that is not gathered by the models is present, introducing an additional element of underestimation. This is combined with the edge effect described above, the plots with higher biomass contains a heightened proportion of tree canopies emerging from the plot boundary.

The additional difference observed in the single tree scheme can be explained by the fact that the model used to estimate the AGB uses as a variable the tree height that is modelled from the CPA. As previously discussed, the bigger crowns are segmented in more than one object; this determines a negative bias in the tree height estimation, something which is proportionally higher at increasing number of subdivisions. To find an approximation for an optimal scale, we applied the root mean square error, as error criterion. Accordingly, the scale defined in the segmentation is the one that minimizes the overall RMSE. Considering that the mode is situated in the lower biomass classes, the selected scale is low; this allows the accurate extraction of the smallest crowns but, as a consequence, splits the bigger canopies in more than one object. This can be seen in figure 24, in which AGB values up to 500 kg are equally distributed along the 1 to 1 line and increasing values are mainly positioned under the line.

A similar trend can be observed in the distribution of the points in the area based approach (fig 25). However, in this case, the predictions are evenly distributed along the 1 to 1 line in the middle range, while they are generally above at the lowest values.

It is necessary to point out that the models were tested in challenging conditions with a very fine scale and taking into account even the smallest trees. As an example, a plot with mean CPA of 1,37 m^2 and tree height of 1m (n=12) is in the sample and its biomass is estimated by the single tree model with an error of 20%.

The AGB estimation at on very fine level is a challenging task due to the increased spectral signature heterogeneity (Lu et al. 2008). Moreover, the assessment of AGB estimation results at a per-pixel level is often difficult, and the accuracy may be misleading due to the registration errors between field collection data and the image (Lu, 2006). In general, the assessment of AGB estimation results can be conducted based on different levels, such as per-pixel level, per-field level or polygon level, and the total amount for the study area (Lu 2006). Several studies have demonstrated that the estimates using high-resolution data have high root mean square error (RMSE) on a pixel level (e.g., Tokola et al., 1996; Trotter et al., 1997). The reliability increases with the area for which mean values are presented (Tokola and Heikkila 1997).

This is confirmed by the means values of the predicted AGB by the different models over the total study area presented in table 8. At this scale, the predicted biomass results are very close to observed values. The mean AGB as estimated from the IFN-CV data for the study area of 14399 ha was 12.701 Mg ha^{-1}. This compared with

11.380 Mg ha^{-1} (APE 10 %) predicted by the area based model and 10.278 Mg ha^{-1} (APE 19 %) predicted by the single tree model.

Model	Observed AGB Mg ha^{-1}	Predicted AGB Mg ha^{-1}	Absolute deviation Mg ha^{-1}	Absolute percentage error (APE) %
Area based model	12.701	12.568	0.1335	1%
Area based spatial	12.701	11.380	1.321	10%
Single tree model	12.701	10.278	2.423	19%
Single tree spatial	12.701	8.891	3.810	30%

Table 8: Comparison between predicted versus observed AGB in the study area (14399 ha)

In summary, the two approaches produced similar results in the overall performance of AGB estimation. In the lowest biomass classes more accurate performance is achieved with the single tree approach. The area based model demonstrates a more uniform prediction, even in the middle range but with higher deviation. Improvements for the area based approach can be reached mainly by improving the image classification, while in the single tree scheme is also possible to improve the predictions by tuning the scale values to better extract the tree crowns.

According to Katila and Tomppo, stratification of the remotely sensed data based on ancillary data are an effective way to improve estimation accuracy within each stratum (Katila and Tomppo, 2001 and 2002).

Thus, the improvement of forest mapping and division in strata, homogeneous per forest type, age, crowns size, ant tree height and the use of different scales in the segmentation can lead to enhanced AGB estimations.

5.1 SOURCES OF ERROR

Several sources of error are associated with the AGB estimation both from ground truth data and form image processing.

Primary sources of error associated with AGB prediction include allometric errors, modeling/measurement errors, and sampling errors (Montesano et al., 2013)

Allometric errors are associated in this study with the relationship between crown width and tree height to AGB. The allometric equation used in this study is quite robust and was developed specifically for Cape Verde and the observed species (n=237; r^2=0.729). Thus, so can be expected that this component is marginally influencing the overall accuracy of reference AGB estimation, where the CPA and all three heights are directly measured in the field.

In the case of AGB predicted by the single tree model, the height is derived by the CPA as independent variable. In this case, the relation between the two parameters is weaker (n=7171; R^2 = 0.533). This introduces an additional source of error in the estimations. In the area based model, the AGB is directly estimated as dependent variable of the CPA. In this case, the relation explains the 70% of variability (n=183; R^2 =0.701). Nevertheless, the results demonstrate similar levels of NRMSE%, both for CPA and AGB estimation, indicating that these factors are not a critical source of uncertainly.

Modeling/measurement errors arise from the relationship of field-measured to remotely sensed data. In this case, the accuracy of tree crown measurements both in the field and from the imagery plays an essential role.

The importance of geometric accuracy of field sample plots and remotely sensed data is obvious because poor geometric accuracy could result in spurious relationships between AGB and the remotely sensed data.

The field data used in this study were collected on the basis of an accurate plot center location and tree position mapping that was realized with a real-time DGPS, electronic compass navigation and laser rangefinder. Considering the data collection technique used, it can be affirmed that the geometric accuracy of field data is assured.

Nevertheless, the measurement of the tree crown projected area in the field is a challenging task that is achieved by an approximation based on four or more points. Taking into account the great irregularity and variability of crown shapes, it is evident that this can be an important source of error that affects the comparison with the remote sensing retrieved data. Moreover, the crown width that is the input in the AGB allometric equation is calculated assuming that the crowns have a circular shape. The associated error becomes greater when the crowns have irregular shapes.

The extraction of the tree crowns from remote sensing data is a critical point in the model. The spectral response of a single tree on remotely sensed images may be affected by the crown shape, yielding brighter sun-facing sides and darker sides facing away from the sun combined with the background. In dark soil, tree canopies tend to be overestimated because parts of the soil are classified in the same cluster of the tree crowns. On the contrary, in the areas with a light soil was observed a loss of crown brighter parts as result of the filtering and reclassifying process. As

discussed above, the proposed method permitted the minimization of the constraints due to poor spectral contrast between the background and tree crowns. However, it was observed that a certain number of the pixels in the lighter and shadowed parts of the scene are misclassified. Additionally, the shadows of the buildings, slopes, rocks and some artificial surfaces have similar signatures to the trees and tend to be classified in the same cluster of the tree canopies, thus introducing uncertainty in the spatialization of the variables over large areas.

The inaccurate segmentation is another important source of error that amplifies the bias in the tree height modeling. As discussed above, in certain cases a single tree canopy is represented by more than one segment and in others cases two or three canopies are grouped in one segment. In this case, a bias is introduced in the AGB estimation.

Another possible source of error in the remotely sensed data is related to CPA calculation where an overlap of crowns layers in denser stands exists.

Finally, the edge effect described above (paragraph 4.5), affects the comparison between observed and predicted data.

Sampling errors occur when points are used to characterize areas. They are a function of the number of observations available, their spatial resolution, and the spatial variability (heterogeneity) of the area being evaluated.

In the present study, taking into account the number of samples observed and the variability of forest structure, it can be affirmed that that this source of error has limited impact on the uncertainty of the final results (table 9 and figure26).

Estimation	ABG Mg ha^{-1}	n	RSE%	Confidence interval $\alpha=0.1$
Study Area (CV-NFI)	12.7	183	5%	10.9 – 14.4

Table 9: Average AGB, confidence interval and relative standard error (RSE %) for the study area.
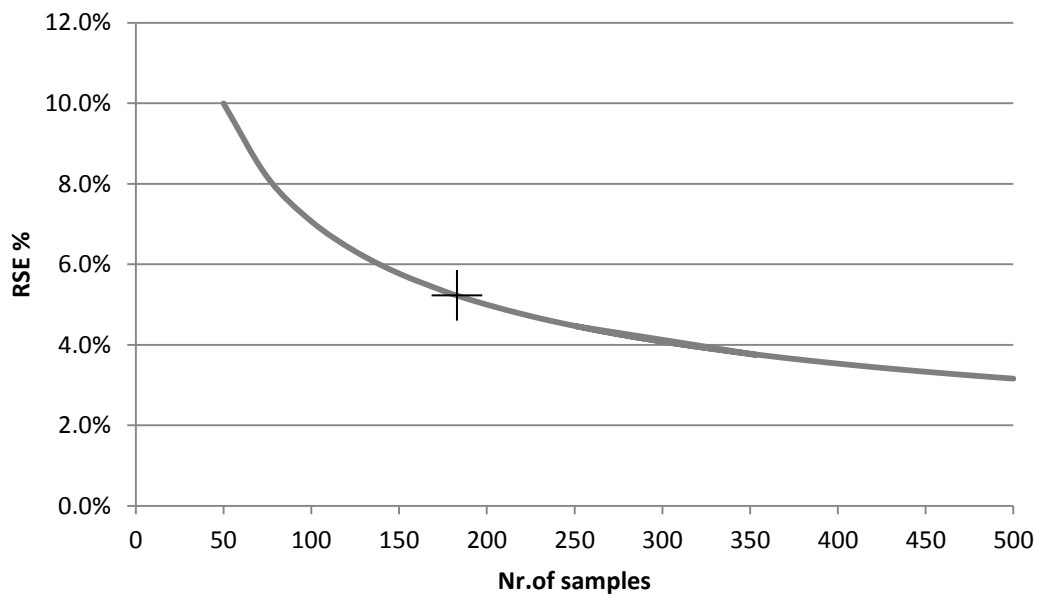
Figure 26: Trend of the relative standard error at increasing number of sampling plots for the observed AGB variability in the study area. The point represents the RSE at the given number of samples in the study area.

5.2   LIMITATIONS AND RECOMMENDATIONS FOR FUTURE INVESTIGATION

The applicability of the proposed method is limited to simple forest stands with no overlap between the crowns.

In the course of this investigation, several research limitations were identified. These can be categorized into two general areas: (1) field data limitations, and (2) remotely sensed data and data processing limitations. As discussed above, the field

data limitations demonstrated have a limited impact and the greatest challenges are identified in tree crown extraction from remote sensing data.

Overall, rather than detracting from the research findings, the limitations identified here represent opportunities for future research. Considering the number of samples involved and the data collection technique, the field data can be considered a representative biomass reference for further analysis and investigation.

A next step should be to test the potential of estimating AGB over areas outside the area from witch ground data were used for deriving models and the accuracy at different scales.

A further improvement of the method should be the stratification of the remotely sensed data on the basis of background characteristics and ancillary data permitting finer tuning during image processing.

Deeper GIS analysis oriented to the elaboration of more detailed forest maps can play a significant role in improving accuracy. This can be the basis for an iterative process of tuning the models and mapping the biomass and forest cover throughout the country. Additional meta-information about forest stands, site characteristics, or species-specific information can be used in the context of this methodology.

Additionally the proposed techniques can be used for change detection in forest cover and biomass over the time.

6. REFERENCES

1. Adams, R.; Bischof, L.,1994. "Seeded region growing," in Pattern Analysis and Machine Intelligence, IEEE Transactions on , vol.16, no.6, pp.641-647

2. Anderson, J. E., L. C. Plourde, M. E. Martin, B. H. Braswell, M. L. Smith, R. O. Dubayah, M. A. Hofton, and J. B. Blair. 2008. "Integrating Waveform Lidar with Hyperspectral Imagery for Inventory of a Northern Temperate Forest." Remote Sensing of Environment 112 (4): 1856–1870. doi:10.1016/j.rse.2007.09.009.

3. Ardila, J.P., Bijker, W., Tolpekin, V.A., Stein, A.,2012. Quantification of crown changes and change uncertainty of trees in an urban environment. ISPRS J. Photogram. Remote Sens. 74, 41–55, http://dx.doi.org/10.1016/j.isprsjprs.2012.08.007.

4. Baccini, A., N. Laporte, S. J. Goetz, M. Sun, and H. Dong. 2008. "A First Map of Tropical Africa's Above-ground Biomass Derived from Satellite Imagery." Environmental Research Letters 3 (4): 045011. doi:10.1088/1748-9326/3/4/045011.

5. Ball, G. H., and Hall, D. J., 1965. A Novel Method of Data Analysis and Pattern Classification. Menlo Park, CA: Stanford Research Institute.

6. Balzter, H., C. S. Rowland, and P. Saich. 2007. "Forest Canopy Height and Carbon Estimation at Monks Wood National Nature Reserve, UK, Using Dual-wavelength SAR Interferometry." Remote Sensing of Environment 108: 224–239. doi:10.1016/j.rse.2006.11.014.

7. Bannari, A., D. Morin, F. Bonn, and A. R. Huete. 1995. "A Review of Vegetation Indices." Remote Sensing Reviews 13: 95–120. doi:10.1080/02757259509532298.

8. Barbati A, Chirici G, Corona P, Montaghi A, Travaglini D. 2009. "Area-based assessment of forest standing volume by field measurements and airborne laser scanner data". Int. J. Remote. Sens. 30 (19): 5177-5194

9. Blackard, J. A., Finco, M. V., Helmer, E. H., Holden, G. R., Hoppus, M. L., Jacobs, D.M., et al. 2008. "Mapping U.S. forest biomass using nationwide forest inventory data and moderate resolution information". Remote Sensing of Environment, 112(4), 1658–1677

10. Blackburn, G.A., Milton, E.J., 1997. An ecological survey of deciduous woodlands using airborne remote sensing and geographical information systems (GIS). Int. J. Remote Sensing 18(9), 1919±1935.

11. Brochmann, C., Rustan, Ø. H. 1987. "Distributional and ecological patterns of the endemic vascular flora of the Cape Verde Islands."Cour. Forsch.-Inst. Senckenberg 95: 155-173

12. Brochmann, C., Rustan, Ø. H., Lobin, W., Kilian, N.1997. "The endemic vascular plants of the Cape Verde Islands, W Africa". Sommerfeltia, 24:1-356. Oslo

13. Brown, S., A. J. R. Gillespie, and A. E. Lugo. 1989. "Biomass Estimation Methods for Tropical Forests with Applications to Forest Inventory Data." Forest Science 35: 881–902.

14. Brown, S., and A. E. Lugo. 1984. "Biomass of Tropical Forests: A New Estimate Based on Forest Volume." Science 223 (4642): 1290–1293. doi:10.1126/science.223.4642.1290.

15. Carreiras, J. M. B., M. J. Vasconcelos, and R. M. Lucas. 2012. "Understanding the Relationship between Aboveground Biomass and ALOS PALSAR Data in the Forests of Guinea-Bissau (West Africa)." Remote Sensing of Environment 121: 426–442. doi:10.1016/j.rse.2012.02.012.

16. Chave, J., M. Réjou-Méchain, A. Búrquez, E. Chidumayo, M. S. Colgan, W. B. C. Delitti, A. Duque, 2014. "Improved Allometric Models to Estimate the Aboveground Biomass of Tropical Trees." Global Change Biology 20 (10): 3177–3190. doi:10.1111/gcb.12629

17. Chen, Q. 2013. "Lidar Remote Sensing of Vegetation Biomass." In: Remote Sensing of Natural Resources, edited by Q. Weng and G. Wang, 399–420. Boca Raton, FL: CRC Press and Taylor & Francis Group.

18. Chen, Q., D. Baldocchi, P. Gong, and M. Kelly. 2006. "Isolating Individual Trees in a Savanna Woodland Using Small Footprint Lidar Data." Photogrammetric Engineering and Remote Sensing 72 (8): 923–932. doi:10.14358/PERS.72.8.923

19. Chen, Q., G. Vaglio Laurin, J. J. Battles, and D. Saah. 2012. "Integration of Airborne Lidar and Vegetation Types Derived from Aerial Photography for Mapping Aboveground Live Biomass." Remote Sensing of Environment 121: 108–117. doi:10.1016/j.rse.2012.01.021.

20. Chirici, G., Barbati, A., Corona, P., Marchetti, M., Travaglini, D., Maselli,F., Bertini R. 2008 "Non-parametric and parametric methods using satellite

images for estimating growing stock volume in alpine and Mediterranean forest ecosystems" Remote Sensing of Environment Volume 112, Issue 5, 15 May 2008, Pages 2686–2700

21. Chirici, G., McRoberts, R., Fattorini, L., Mura M., Marchetti, M., 2016."Comparing echo-based and canopy height model-based metrics for enhancing estimation of forest aboveground biomass in a model-assisted framework" Remote Sensing of Environment 174: 1–9

22. Cienciala, E.; Centeio, A.; Blazek, P.; Soares, M.C.G.; Russ, R. 2013."Estimation of stem and tree level biomass models for Prosopis juliflora/pallid applicable to multi-stemmed tree species". Trees, 27(4):1061-1070. DOI: 10.1007/s00468-013-0857-1

23. Clark, M. L., D. A. Roberts, J. J. Ewel, and D. B. Clark. 2011. "Estimation of Tropical Rain Forest Aboveground Biomass with Small-footprint Lidar and Hyperspectral Sensors." Remote Sensing of Environment 115: 2931–2942. doi:10.1016/j.rse.2010.08.029.

24. Cloude, S. R., and K. P. Papathanassiou. 2003. "Three-stage Inversion Process for Polarimetric SAR Interferometry." IEE Proceedings Radar, Sonar and Navigation 150: 125–134. doi:10.1049/ip-rsn:20030449.

25. Congalton, R. G. 2001. "Accuracy Assessment and Validation of Remotely Sensed and Other Spatial Information."International Journal of Wildland Fire 10: 321–328. doi:10.1071/WF01031.

26. Congalton, R. G., and K. Green. 2009. Assessing the Accuracy of Remotely Sensed Data: Principles and Practices. 2nd ed. Boca Raton, FL: CRC Press.

27.

28. Corona P, Fattorini L. 2008. "Area-based LiDAR-assisted estimation of forest standing volume". Can. J. For. Res. 38(11): 2911-2916

29. DeGrandi, G. D., R. M. Lucas, and J. Kropacek. 2009. "Analysis by Wavelet Frames of Spatial Statistics in SAR Data for Characterizing Structural Properties of Forests." IEEE Transactions on Geoscience and Remote Sensing 47: 494–507. doi:10.1109/TGRS.2008.2006183.

30. Dobson, M. C., F. T. Ulaby, L. E. Pierce, T. L. Sharik, K. M. Bergen, J. Kellndorfer, J. R. Kendra, et al. 1995. "Estimation of Forest Biomass Characteristics in Northern Michigan with SIR-C/XSAR Data." IEEE Transactions on Geoscience and Remote Sensing 33: 877–894. doi:10.1109/36.406674.

31. Dralle, K.; Rudemo, M. 1996. "Stem number estimation by kernel smoothing of aerial photos" Can. J. For. Res 26, 1228–1236.

32. Du, L., T. Zhou, Z. Zou, X. Zhao, K. Huang, and H. Wu. 2014. "Mapping Forest Biomass Using Remote Sensing and National Forest Inventory Data." Forests 5: 1267–1283.

33. Foody, G.M., 2003, Remote sensing of tropical forest environments: towards the monitoring of environmental resources for sustainable development. International Journal of Remote Sensing, 24, pp. 4035–4046.

34. García, M., D. Riaño, E. Chuvieco, and F. M. Danson. 2010. "Estimating Biomass Carbon Stocks for a Mediterranean Forest in Central Spain Using LiDAR Height and Intensity Data." Remote Sensing of Environment 114: 816–830.

35. García, M., S. Popescu, D. Riaño, K. Zhao, A. Neuenschwander, M. Agca, and E. Chuvieco. 2012. "Characterization of Canopy Fuels Using ICESat/GLAS Data." Remote Sensing of Environment 123: 81–89.

36. Garestier, F., and T. Le Toan. 2010. "Forest Modeling for Height Inversion Using Single-baseline InSAR/Pol-InSAR Data." IEEE Transactions on Geoscience and Remote Sensing 48 (3): 1528–1539. doi:10.1109/TGRS.2009.2032538.

37. Gärtner, P., Förster, M.,Kurbanb,A., Kleinschmit, B., 2014. "Object based change detection of Central Asian Tugai vegetation with very high spatial resolution satellite imagery"International Journal of Applied Earth Observation and Geoinformation 31: 110–121

38. Gitelson, A. A., Y. J. Kaufman, R. Stark, and D. Rundquist, 2002 "Novel algorithms for remote estimation of vegetation fraction". Remote Sens. Environ.,80 76–87

39. Gleason, C. J., and J. Im. 2011. "A Review of Remote Sensing of Forest Biomass and Biofuel: Options for Small-area Applications." GIScience & Remote Sensing 48 (2): 141–170. doi:10.2747/1548-1603.48.2.141.

40. Goetz, S., A. Baccini, N. Laporte, T. Johns, W. Walker, J. Kellndorfer, R. Houghton, and M. Sun. 2009. "Mapping and Monitoring Carbon Stocks with Satellite Observations: A Comparison of Methods." Carbon Balance and Management 4 (2): 1–7.

41. Greer, J.D., 1993." The view from above". J. Forestry 8, 10±14.

42. Gupta S., Weinacker H.,and Koch B. 2010. "Comparative Analysis of Clustering-Based Approaches for 3-D Single Tree Detection Using Airborne Fullwave Lidar Data". Remote Sensing 2, 968-989.

43. Hame, T., A. Salli, K. Andersson, and A. Lohi. 1997. "A New Methodology for the Estimation of Biomass of Conifer Dominated Boreal Forest Using NOAA AVHRR Data." International Journal of Remote Sensing 18: 3211–3243. doi:10.1080/014311697217053.

44. Henry, M., A. Besnard, W. A. Asante, J. Eshun, S. Adu-Bredu, R. Valentini, M. Bernoux, and L. Saint-André. 2010. "Wood Density, Phytomass Variations within and among Trees, and Allometric Equations in a Tropical Rainforest of Africa." Forest Ecology and Management 260 (8): 1375–1388. doi:10.1016/j.foreco.2010.07.040

45. Holmgren, P., Thuresson, T., Holm, S., 1997. Estimating forest characteristics in scanned aerial photographs with respect to requirements for economic forest management planning. Scand. J. For. Res. 12, 189±199

46. Holopainen, M., Lukkarinen, E., 1994. " Digital aerial photographs in forest inventory". Department of Forest Resource Management Publications, University of Helsinki, vol. 4, pp. 1± 33.

47. Huang, Y. P., and J. S. Chen. 2013. "Advances in the Estimation of Forest Biomass Based on SAR Data." Remote Sensing for Land and Resources 25: 7–13.

48. Hudak, A. T., E. K. Strand, L. A. Vierling, J. C. Byrne, J. U. H. Eitel, S. Martinuzzi, and M. J. Falkowski. 2012. "Quantifying Aboveground Forest

Carbon Pools and Fluxes from Repeat LiDAR Surveys." Remote Sensing of Environment 123: 25–40. doi:10.1016/j.rse.2012.02.023.

49. Hyde, P., R. Dubayah, W. Walker, J. B. Blair, M. Hofton, and C. Hunsaker. 2006. "Mapping Forest Structure for Wildlife Habitat Analysis Using Multi-sensor (LiDAR, SAR/InSAR, ETM+, QuickBird) Synergy." Remote Sensing of Environment 102: 63–73. doi:10.1016/j.rse.2006.01.021

50. Hyyppä, J., Inkinen, M., 1999. Detecting and estimating attributes for single trees using laser scanner. The Photogrammetric Journal of Finland, 16, pp. 27-42

51. Kasischke, E. S., J. M. Melack, and M. C. Dobson. 1997. "The Use of Imaging Radars for Ecological Applications: A Review."Remote Sensing of Environment 59 (2): 141–156. doi:10.1016/S0034-4257(96)00148-4.

52. Katila, M. and Tomppo, E., 2001, Selecting estimation parameters for the Finnish multisource national forest inventory. Remote Sensing of Environment, 76, pp. 16–32

53. Katila, M.,Tomppo,E., 2002 "Stratification by ancillary data in multisource forest inventories employing k-nearest-neighbour estimation". Canadian Journal of Forest Research, 2002, 32(9): 1548-1561, 10.1139/x02-047

54. Katoh, M., Gougeon, F.A., 2012. "Improving the precision of tree counting by combining tree detection with crown delineation and classification on homogeneity guided smoothed high resolution (50 cm) multispectral airborne digital data". Remote Sens. 4, 1411–1424, http://dx.doi.org/10.3390/rs4051411

55. Kayitakire, F., C. Hamel, and P. Defourny. 2006. "Retrieving Forest Structure Variables Based on Image Texture Analysis and IKONOS-2 Imagery." Remote Sensing of Environment 102 (3–4): 390–401. doi:10.1016/j.rse.2006.02.022.

56. Ke, Y., Quackenbush, L.J., 2011a. "A comparison of three methods for automatic tree crown detection and delineation from high spatial resolution imagery". Int. J. Remote Sens. 32, 3625–3647, http://dx.doi.org/10.1080/01431161003762355.

57. Ke, Y., Quackenbush, L.J., 2011b. "A review of methods for automatic individual treecrown detection and delineation from passive remote sensing". Int. J. Remote Sens. 32, 4725–4747, http://dx.doi.org/10.1080/01431161.2010.494184

58. Kellndorfer, J. M., W. S. Walker, E. LaPoint, K. Kirsch, J. Bishop, and G. Fiske. 2010. "Statistical Fusion of Lidar, InSAR, and Optical Remote Sensing Data for Forest Stand Height Characterization: A Regional-scale Method Based on LVIS, SRTM, Landsat ETM+, and Ancillary Data Sets." Journal of Geophysical Research 115: G00E08. doi:10.1029/2009JG000997.

59. Kellndorfer, J., W. Walker, L. Pierce, C. Dobson, J. A. Fites, C. Hunsaker, J. Vona, and M. Clutter. 2004. "Vegetation Height Estimation from Shuttle Radar Topography Mission and National Elevation Datasets." Remote Sensing of Environment 93 (3): 339–358. doi:10.1016/j.rse.2004.07.017

60. Klinge, H., W. A. Rodriguez, E. Brunig, and E. J. Fittkau. 1975. "Biomass and Structure in a Central Amazônian Rain Forest."In Tropical Ecological Systems: Trends in Terrestrial and Aquatic Research, edited by F. B. Golley and E. Medina, 115–122. Berlin: Springer-Verlag

61. Koch, B.; Heyder, U.; Weinacker, H. Detection of individual tree crowns in airborne lidar data. Photogramm. Eng. Remote Sens. 2006, 72, 357-363. 8.

62. Kuplich, T. M., P. J. Curran, and P. M. Atkinson. 2005. "Relating SAR Image Texture to the Biomass of Regenerating Tropical Forests." International Journal of Remote Sensing 26 (21): 4829–4854. doi:10.1080/01431160500239107.

63. Latifi, H., F. Fassnacht, and B. Koch. 2012. "Forest Structure Modeling with Combined Airborne Hyperspectral and LiDAR Data." Remote Sensing of Environment 121: 10–25. doi:10.1016/j.rse.2012.01.015.

64. Le Toan, T., A. Beaudoin, and D. Guyon. 1992. "Relating Forest Biomass to SAR Data." IEEE Transactions on Geoscience and Remote Sensing 30 (2): 403–411. doi:10.1109/36.134089.

65. Le Toan, T., S. Quegan, M. W. J. Davidson, H. Balzter, P. Paillou, K. Papathanassiou, S. Plummer, et al. 2011. "The BIOMASS Mission: Mapping Global Forest Biomass to Better Understand the Terrestrial Carbon Cycle." Remote Sensing of Environment115 (11): 2850–2860. doi:10.1016/j.rse.2011.03.020.

66. Leboeuf, A., A. Beaudoin, R. A. Fournier, L. Guindon, J. E. Luther, and M. C. Lambert. 2007. "A Shadow Fraction Method for Mapping Biomass of Northern Boreal Black Spruce Forests Using QuickBird Imagery." Remote Sensing of Environment 110 (4): 488–500. doi:10.1016/j.rse.2006.05.025.

67. Leckie, D.G. 1990 "Advances in remote sensing technologies for forest surveys and management" Canadian Journal of Forest Research 20(4): 464-483.

68. Lefsky, M. A., D. J. Harding, M. Keller, W. B. Cohen, C. C. Carabajal, F. Del Bom Espirito-Santo, M. O. Hunter, and R. de Oliveira. 2005. "Estimates of Forest Canopy Height and Aboveground Biomass Using ICESat." Geophysical Research Letters 32: L22S02

69. Lehtonen, A., R. Mäkipää, J. Heikkinen, R. Sievänen, and J. Liski. 2004. "Biomass Expansion Factors (BEFs) for Scots Pine, Norway Spruce and Birch According to Stand Age for Boreal Forests." Forest Ecology and Management 188 (1–3): 211–224. doi:10.1016/j.foreco.2003.07.008.

70. Li, G., D. Lu, E. Moran, L. Dutra, and M. Batistella. 2012. "A Comparative Analysis of ALOS PALSAR L-band and RADARSAT-2 C-band Data for Land-cover Classification in a Tropical Moist Region." ISPRS Journal of Photogrammetry and Remote Sensing70: 26–38. doi:10.1016/j.isprsjprs.2012.03.010.

71. Lim, K., P. Treitz, K. Baldwin, I. Morrison, and J. Green. 2003. "Lidar Remote Sensing of Biophysical Properties of Tolerant Northern Hardwood Forests." Canadian Journal of Remote Sensing 29 (5): 658–678. doi:10.5589/m03-025.

72. Lu, D. 2005. "Aboveground Biomass Estimation Using Landsat TM Data in the Brazilian Amazon." International Journal of Remote Sensing 26: 2509–2525. doi:10.1080/01431160500142145.

73. Lu, D. 2006. "The Potential and Challenge of Remote Sensing-based Biomass Estimation." International Journal of Remote Sensing 27 (7): 1297–1328. doi:10.1080/01431160500486732.

74. Lu, D., and M. Batistella. 2005. "Exploring TM Image Texture and Its Relationships with Biomass Estimation in Rondônia, Brazilian Amazon." Acta Amazonica 35 (2): 249–257. doi:10.1590/S0044-59672005000200015.

75. Lu, D., M. Batistella, and E. Moran. 2005. "Satellite Estimation of Aboveground Biomass and Impacts of Forest Stand Structure." Photogrammetric Engineering and Remote Sensing 71 (8): 967–974. doi:10.14358/PERS.71.8.967.

76. Lu, D., P. Mausel, E. Brondízio, and E. Moran. 2004. "Relationships between Forest Stand Parameters and Landsat TM Spectral Responses in the Brazilian Amazon Basin." Forest Ecology and Management 198 (1–3): 149–167. doi:10.1016/j.foreco.2004.03.048

77. Lu, D., Q. Chen, G. Wang, E. Moran, M. Batistella, M. Zhang, G. Vaglio Laurin, and D. Saah. 2012. "Aboveground Forest Biomass Estimation with Landsat and LiDAR Data and Uncertainty Analysis of the Estimates." International Journal of Forestry Research 2012: 16. doi:10.1155/2012/436537.

78. Lu, D., Q. Chen, G. Wang, E. Moran, M. Batistella, M. Zhang, G. Vaglio Laurin, and D. Saah. 2012. "Aboveground Forest Biomass Estimation with Landsat and LiDAR Data and Uncertainty Analysis of the Estimates." International Journal of Forestry Research 2012: 16. doi:10.1155/2012/436537.

79. Lu,D., Chen,Q., Wang,G Liu, L., Li,G., & Moran,E. 2014. "A survey of remote sensing-based aboveground biomass estimation methods in forest ecosystems". International Journal of Digital Earth, DOI: 10.1080/17538947.2014.990526

80. Maselli,F., Chirici,G., Bottai,L., Corona,P., Marchetti,M. 2005. "Estimation of Mediterranean forest attributes by the application of k-NN procedures to multitemporal Landsat ETM+ images". International Journal of Remote Sensing. Volume 26, Issue 17, 2005. DOI:10.1080/01431160500166433

81. McDonald, A. J., F. M. Gemmell, and P. E. Lewis. 1998. "Investigation of the Utility of Spectral Vegetation Indices for Determining Information on Coniferous Forests." Remote Sensing of Environment 66 (3): 250–272. doi:10.1016/S0034-4257(98)00057-1.

82. McRoberts, R. E., E. Næsset, and T. Gobakken. 2013. "Inference for Lidar-assisted Estimation of Forest Growing Stock Volume." Remote Sensing of Environment 128: 268–275. doi:10.1016/j.rse.2012.10.007.

83. Means, J. E., S. A. Acker, D. J. Harding, J. B. Blair, M. A. Lefsky, W. B. Cohen, M. E. Harmon, and W. A. McKee. 1999. "Use of Large-footprint Scanning Airborne Lidar to Estimate Forest Stand Characteristics in the Western Cascades of Oregon." Remote Sensing of Environment 67 (3): 298–308. doi:10.1016/S0034-4257(98)00091-1.

84. Migliavacca, M., Galvagno, M., Cremonese,E., Rossini,M., Meroni, M., Sonnentage, O., Cogliati,S., Manca, G., Diotri,F., Busetto, L., Cescattia,A., Colombo, R., Fava, F., Morra di Cella,U., Pari,E., Siniscalco,C., Richardson A, 2011. "Using digital repeat photography and eddy covariance data to model grassland phenology and photosynthetic CO2 uptake". Agricultural and Forest Meteorology 151: 1325–1337.

85. Miller, M. E., M. Lefsky, and Y. Pang. 2011. "Optimization of Geoscience Laser Altimeter System Waveform Metrics to Support Vegetation

Measurements." Remote Sensing of Environment 115 (2): 298–305. doi:10.1016/j.rse.2010.09.002

86. Mitchard, E. T. A., S. S. Saatchi, S. L. Lewis, T. R. Feldpausch, I. H. Woodhouse, B. Sonké, C. Rowland, and P. Meir. 2011. "Measuring Biomass Changes Due to Woody Encroachment and Deforestation/degradation in a Forest–savanna Boundary Region of Central Africa Using Multi-temporal L-band Radar Backscatter." Remote Sensing of Environment 115 (11): 2861–2873. doi:10.1016/j.rse.2010.02.022.

87. Montesano, P. M., B. D. Cook, G. Sun, M. Simard, R. F. Nelson, K. J. Ranson, Z. Zhang, and S. Luthcke. 2013. "Achieving Accuracy Requirements for Forest Biomass Mapping: A Spaceborne Data Fusion Method for Estimating Forest Biomass and LiDAR Sampling Error." Remote Sensing of Environment 130: 153–170. doi:10.1016/j.rse.2012.11.016.

88. Morsdorf, F.; Meier, E.; Kötz, B.; Itten, K.I. Lidar based geometric reconstruction of boreal type forest stands at single tree level for forest and wildland fire management. Remote Sens. Environ. 2004, 92, 353-362.

89. Muukkonen, P., and J. Heiskanen. 2007. "Biomass Estimation Over a Large Area Based on Standwise Forest Inventory Data and ASTER and MODIS Satellite Data: A Possibility to Verify Carbon Inventories." Remote Sensing of Environment 107 (4): 617–624. doi:10.1016/j.rse.2006.10.011.

90. Næsset, E., T. Gobakken, O. M. Bollandsås, T. G. Gregoire, R. Nelson, and G. Ståhl. 2013. "Comparison of Precision of Biomass Estimates in Regional Field Sample Surveys and Airborne LiDAR-assisted Surveys in Hedmark County, Norway."Remote Sensing of Environment 130: 108–120.

91. Næsset, E., T. Gobakken, S. Solberg, T. G. Gregoire, R. Nelson, G. Ståhl, and D. J. Weydahl. 2011. "Model-assisted Regional Forest Biomass Estimation Using LiDAR and InSAR as Auxiliary Data: A Case Study from a Boreal Forest Area." Remote Sensing of Environment 115: 3599–3614.

92. Nafiseh, G., S. M. Reza, and M. Ali. 2011. "A Review on Biomass Estimation Methods Using Synthetic Aperture Radar Data." International Journal of Geomatics and Geosciences 1: 776–788.

93. Nelson, B. W., R. Mesquita, J. L. G. Pereira, S. G. A. De Souza, G. T. Batista, and L. B. Couto. 1999. "Allometric Regression for Improved Estimate of Secondary Forest Biomass in the Central Amazon." Forest Ecology and Management 117 (1–3): 149–167. doi:10.1016/S0378-1127(98)00475-7.

94. Nelson, R. 2010. "Model Effects on GLAS-based Regional Estimates of Forest Biomass and Carbon." International Journal of Remote Sensing 31 (5): 1359–1372. doi:10.1080/01431160903380557.

95. Nelson, R., K. J. Ranson, G. Sun, D. S. Kimes, V. Kharuk, and P. Montesano. 2009. "Estimating Siberian Timber Volume Using MODIS and ICESat/GLAS." Remote Sensing of Environment 113 (3): 691–701. doi:10.1016/j.rse.2008.11.010.

96. Nelson, R., T. Gobakken, E. Næsset, T. G. Gregoire, G. Ståhl, S. Holm, and J. Flewelling. 2012. "Lidar Sampling-using an Airborne Profiler to Estimate Forest Biomass in Hedmark County, Norway." Remote Sensing of Environment 123: 563–578. doi:10.1016/j.rse.2011.10.036.

97. Ni, W., K. J. Ranson, Z. Zhang, and G. Sun. 2014. "Features of Point Clouds Synthesized from Multi-view ALOS/PRISM Data and Comparisons with LiDAR

Data in Forested Areas." Remote Sensing of Environment 149: 47–57. doi:10.1016/j.rse.2014.04.001.

98. Overman, J. P. M., H. J. L. Witte, and J. G. Saldarriaga. 1994. "Evaluation of Regression Models for Above-ground Biomass Determination in Amazon Rainforest." Journal of Tropical Ecology 10 (02): 207–218. doi:10.1017/S0266467400007859

99. Persson, A.; Holmgren, J.; Söderman, U.2002." Detecting and measuring individual trees using an airborne laser scanner". Photogramm. Eng. Remote Sens. 68, 925-932. 7.

100. Pflugmacher, D., W. B. Cohen, R. E. Kennedy, and Z. Yang. 2014. "Using Landsat-derived Disturbance and Recovery History and Lidar to Map Forest Biomass Dynamics." Remote Sensing of Environment 151: 124–137. doi:10.1016/j.rse.2013.05.033.

101. Popescu, S. C., K. Zhao, A. Neuenschwander, and C. Lin. 2011. "Satellite Lidar vs. Small Footprint Airborne Lidar: Comparing the Accuracy of Aboveground Biomass Estimates and Forest Structure Metrics at Footprint Level." Remote Sensing of Environment 115 (11): 2786–2797. doi:10.1016/j.rse.2011.01.026.

102. Popescu, S. C., R. H. Wynne, and R. F. Nelson. 2002. "Estimating Plot-level Tree Heights with Lidar: Local Filtering with a Canopy-height Based Variable Window Size." Computers and Electronics in Agriculture 37 (13): 71–95. doi:10.1016/S0168-1699(02)00121-7.

103. Popescu, S. C., R. H. Wynne, and R. F. Nelson. 2003. "Measuring Individual Tree Crown Diameter with Lidar and Assessing Its Influence on

Estimating Forest Volume and Biomass. Canadian Journal of Remote Sensing 29 (5): 564–577. doi:10.5589/m03-027.

104.   Rahman, M. M., and J. T. S. Sumantyo. 2013. "Retrieval of Tropical Forest Biomass Information from ALOS PALSAR Data."Geocarto International 28 (5): 382–403. doi:10.1080/10106049.2012.710652.

105.   Rivington, M., K. B. Matthews, G. Bellocchi, and Buchan, K., 2006. "Evaluating Uncertainty Introduced to Process-based Simulation Model Estimates by Alternative Sources of Meteorological Data." Agricultural Systems 88 (2–3): 451–471. doi:10.1016/j.agsy.2005.07.004.

106.   Saatchi, S. S., N. L. Harris, S. Brown, M. Lefsky, E. T. A. Mitchard, W. Salas, B. R. Zutta, et al. 2011b. "Benchmark Map of Forest Carbon Stocks in Tropical Regions Across Three Continents." Proceedings of the National Academy of Sciences 108 (24): 9899–9904. doi:10.1073/pnas.1019576108.

107.   Sandberg, G., L. M. H. Ulander, J. E. S. Fransson, J. Holmgren, and T. Le Toan. 2011. "L- and P-band Backscatter Intensity for Biomass Retrieval in Hemiboreal Forest." Remote Sensing of Environment 115 (11): 2874–2886. doi:10.1016/j.rse.2010.03.018.

108.   Santos, J. R., M. S. P. Lacruz, L. S. Araujo, and M. Keil. 2002. "Savanna and Tropical Rainforest Biomass Estimation and Spatialization Using JERS-1 data." International Journal of Remote Sensing 23 (7): 1217–1229. doi:10.1080/01431160110092867

109.   Sarker, M. L. R., J. Nichol, B. Ahmad, I. Busu, and A. A. Rahman. 2012. "Potential of Texture Measurements of Two-date Dual Polarization PALSAR Data for the Improvement of Forest Biomass Estimation." ISPRS Journal of

Photogrammetry and Remote Sensing 69: 146–166. doi:10.1016/j.isprsjprs.2012.03.002.

110. Segura, M., and M. Kanninen. 2005. "Allometric Models for Tree Volume and Total Aboveground Biomass in a Tropical Humid Forest in Costa Rica." Biotropica 37 (1): 2–8. doi:10.1111/j.1744-7429.2005.02027.x.

111. Seidel, D., S. Fleck, C. Leuschner, and T. Hammett. 2011. "Review of Ground-based Methods to Measure the Distribution of Biomass in Forest Canopies." Annals of Forest Science 68 (2): 225–244.

112. Selkowitz, D. J., G. Green, B. Peterson, and B. Wylie. 2012. "A Multi-sensor Lidar, Multi-spectral and Multi-angular Approach for Mapping Canopy Height in Boreal Forest Regions." Remote Sensing of Environment 121: 458–471. doi:10.1016/j.rse.2012.02.020.

113. Shih, F.Y., Cheng, S.: Automatic seeded region growing for color image segmentation. Image and Vision Computing 23, 877–886 (2005)

114. Silva de Carvalho, M. L., 1994. "Técnicas de conservação de solos em Cabo Verde". DGASP, Praia, Cabo Verde

115. Simard, M., V. H. Rivera-Monroy, J. E. Mancera-Pineda, E. Castañeda-Moya, and R. R. Twilley.2008. "A Systematic Method for 3D Mapping of Mangrove Forests Based on Shuttle Radar Topography Mission Elevation Data, ICEsat/GLAS Waveforms and Field Data: Application to Ciénaga Grande de Santa Marta, Colombia." Remote Sensing of Environment 112 (5): 2131–2144. doi:10.1016/j.rse.2007.10.012.

116. Skowronski, N. S., and A. J. Lister. 2012. "Utility of LiDAR for Large Area Forest Inventory Applications." In Moving from Status to Trends: Forest

Inventory and Analysis (FIA) Symposium, edited by R. S. Morin and Greg C. Liknes, 410–413. Baltimore MD: Gen. Tech. Rep. NRS

117.   Skowronski, N. S., K. L. Clark, M. Gallagher, R. A. Birdsey, and J. L. Hom. 2014. "Airborne Laser Scanner-assisted Estimation of Aboveground Biomass Change in a Temperate Aak–pine Forest." Remote Sensing of Environment 151: 166–174. doi:10.1016/j.rse.2013.12.015.

118.   Smyth, C., W. Kurz, E. Neilson, and G. Stinson. 2013. "National-scale Estimates of Forest Root Biomass Carbon Stocks and Associated Carbon Fluxes in Canada." Global Biogeochemical Cycles 27 (4): 1262–1273. doi:10.1002/2012GB004536.

119.   Solberg, S., R. Astrup, T. Gobakken, E. Naesset, and D. J. Weydahl. 2010. "Estimating Spruce and Pine Biomass with Interferometric X-Band SAR." Remote Sensing of Environment 114 (10): 2353–2360. doi:10.1016/j.rse.2010.05.011.

120.   Steinmann, K., Mandallaz D., Ginzler, C., Lanz, A.(2012) "Small area estimations of proportion of forest and timber volume combining Lidar data and stereo aerial images with terrestrial data" Scandinavian Journal of Forest Research

121.   St-Onge, B., Y. Hu, and C. Vega. 2008. "Mapping the Height and Above-ground Biomass of a Mixed Forest Using Lidar and Stereo Ikonos Images." International Journal of Remote Sensing 29 (5): 1277–1294. doi:10.1080/01431160701736505.

122.   Sun, G., K. J. Ranson, Z. Guo, Z. Zhang, P. Montesano, and D. Kimes. 2011. "Forest Biomass Mapping from Lidar and Radar

Synergies." Remote Sensing of Environment 115 (11): 2906–2916. doi:10.1016/j.rse.2011.03.021.

123. Thenkabail, P. S., N. Stucky, B. W. Griscom, M. S. Ashton, J. Diels, B. van der Meer, and E. Enclona. 2004. "Biomass Estimations and Carbon Stock Calculations in the Oil Palm Plantations of African Derived Savannas Using IKONOS Data."International Journal of Remote Sensing 25: 5447–5472. doi:10.1080/01431160412331291279.

124. Tian, X., Z. Su, E. Chen, Z. Li, C. van der Tol, J. Guo, and Q. He. 2012. "Estimation of Forest Above-ground Biomass Using Multi-parameter Remote Sensing Data Over a Cold and Arid Area." International Journal of Applied Earth Observation and Geoinformation 14 (1): 160–168. doi:10.1016/j.jag.2011.09.010.

125. Tokola, T. & Heikkilä, J. 1997. Improving satellite image based forest inventory by using a priori site quality information. Silva Fennica 31(1): 67–78.

126. Tokola,T., J. Pitkänen, S. Partinen, E. Muinonen 1996 "Point accuracy of a non-parametric method in estimation of forest characteristics with different satellite materials"International Journal of Remote Sensing, Vol. 17, No. 12. (1996), pp. 2333-2351, doi:10.1080/01431169608948776

127. Trotter, J. R. Dymond & C. J. Goulding 1997."Estimation of timber volume in a coniferous plantation forest using Landsat TM"International Journal of Remote Sensing, Volume 18, Issue 10, pages 2209-2223, DOI:10.1080/014311697217846

128.   Tsui, O. W., N. C. Coops, M. A. Wulder, and P. L. Marshall. 2013. "Integrating Airborne LiDAR and Space-borne Radar Via Multivariate Kriging to Estimate Above-ground Biomass." Remote Sensing of Environment 139: 340–352. doi:10.1016/j.rse.2013.08.012.

129.   Tuominen S., Haapanen R. (2013)." Estimation of forest biomass by means of genetic algorithmbased optimization of airborne laser scanning and digital aerial photograph features". Silva Fennica vol. 47 no. 1 article id 902. 20 p.

130.   Uuttera, J. Haara,A., Tokola,T., Maltamo,M.1998. "Determination of the spatial distribution of trees from digital aerial photographs" Forest Ecology and Management 110 275-282

131.   Vaglio Laurin, G., Q. Chen, J. A. Lindsell, D. A. Coomes, F. Frate, L. Del Guerriero, F. Pirotti, and R. Valentini. 2014. "Aboveground Biomass Estimation in an African Tropical Forest with Lidar and Hyperspectral Data." ISPRS Journal of Photogrammetry and Remote Sensing 89: 49–58. doi:10.1016/j.isprsjprs.2014.01.001.

132.   Vanamburg,L. K. ,Trlica, M. J. Hoffer R. M. & Weltz M. A. 2006: "Ground based digital imagery for grassland biomass estimation". International Journal of Remote Sensing Volume 27, Issue 5, 2006

133.   Vauhkonen, J.; Tokola, T.; Packalén, P.; Maltamo, M. Identification of Scandinavian commercial species of individual trees from airborne laser scanning data using alpha shape metrics. For. Science 2009, 55, 37-47. Remote Sens. 2010, 2 988 5.

134.   Walker, W. S., J. M. Kellndorfer, E. LaPoint, M. Hoppus, and J. Westfall. 2007. "An Empirical InSAR-optical Fusion Approach to Mapping Vegetation Canopy Height." Remote Sensing of Environment 109 (4): 482–499. doi:10.1016/j.rse.2007.02.001

135.   Wang, G., and G. Z. Gertner. 2013. "Spatial Uncertainty Analysis When Mapping Natural Resources Using Remotely Sensed Data." In Remote Sensing of Natural Resources, edited by G. Wang and Q. Weng, 89–112. Boca Raton, FL: CRC Press, Taylor & Francis Group.

136.   Wang, G., M. Zhang, G. Z. Gertner, T. Oyana, R. E. McRoberts, and H. Ge. 2011. "Uncertainties of Mapping Aboveground Forest Carbon Due to Plot Locations Using National Forest Inventory Plot and Remotely Sensed Data." Scandinavian Journal of Forest Research 26 (4): 360–373.

137.   Wang, G., T. Oyana, M. Zhang, S. Adu-Prah, S. Zeng, H. Lin, and J. Se. 2009. "Mapping and Spatial Uncertainty Analysis of Forest Vegetation Carbon by Combining National Forest Inventory Data and Satellite Images." Forest Ecology and Management258 (7): 1275–1283. doi:10.1016/j.foreco.2009.06.056.

138.   Zhang, L., G. Yu, F. Gu, H. He, L. M. Zhang, and S. Han. 2012. "Uncertainty Analysis of Modeled Carbon Fluxes for a Broad-leaved Korean Pine Mixed Forest Using a Process-based Ecosystem Model." Journal of Forest Research 17 (3): 268–282. doi:10.1007/s10310-011-0305-2.

139.   Zhao, K., S. Popescu, and R. Nelson. 2009. "Lidar Remote Sensing of Forest Biomass: A Scale-invariant Estimation Approach Using Airborne

Lasers." Remote Sensing of Environment 113 (1): 182–196. doi:10.1016/j.rse.2008.09.009.

140.   Zhen, Z., L. J. Quackenbush, and L. Zhang. 2014. "Impact of Tree-oriented Growth Order in Marker-controlled Region Growing for Individual Tree Crown Delineation Using Airborne Laser Scanner (ALS) Data." Remote Sensing 6 (1): 555–579. doi:10.3390/rs6010555.

141.   Zheng, D., J. Rademacher, J. Chen, T. Crow, M. Bresee, J. Le Moine, and S. Ryu. 2004. "Estimating Aboveground Biomass Using Landsat 7 ETM+ Data Across a Managed Landscape in Northern Wisconsin, USA." Remote Sensing of Environment 93 (3): 402–411. doi:10.1016/j.rse.2004.08.008.

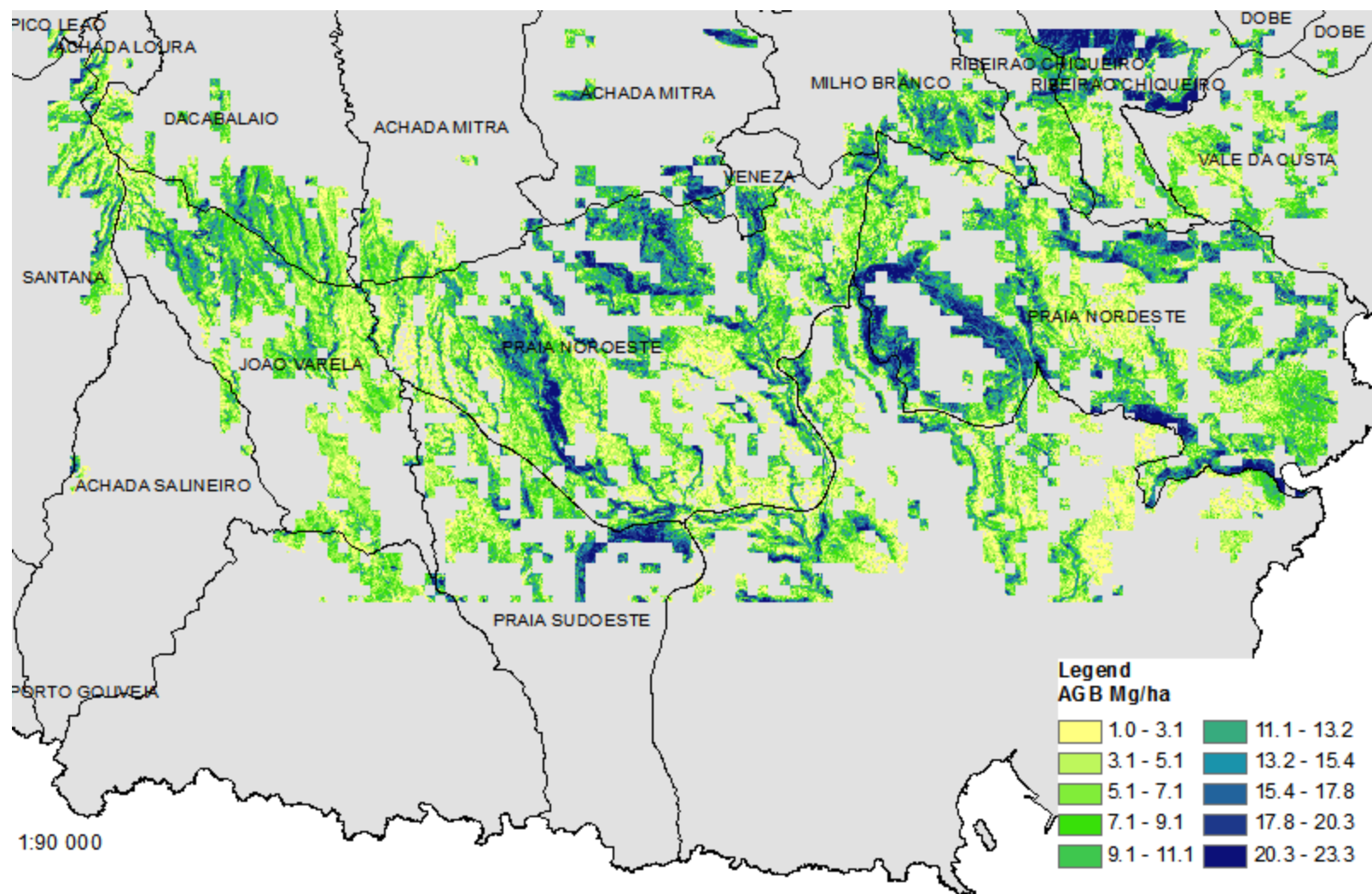**Figure 27:** AGB map of the study area expressed in Mg Ha^{-1}